ELSEVIER

Physica D 119 (1998) 352–380

PHYSICA D

Finite time transport in aperiodic flows ★

G. Haller *, A.C. Poje

Division of Applied Mathematics, Brown University, Providence, RI 02906, USA

Received 12 June 1997; accepted 12 September 1997
Communicated by P. Kolodner

Abstract

We study the transport of particles in a general, two-dimensional, incompressible flow in the presence of a transient eddy, i.e., a bounded set of closed streamlines with a finite time of existence. Using quantities obtained from Eulerian observations, we provide explicit conditions for the existence of a hyperbolic structure in the flow, which induces mixing between the eddy and its environment. Our results can be used directly to study finite-time transport in numerically or experimentally generated vector fields with general time-dependence. © 1998 Elsevier Science B.V.

1. Introduction

The transport of fluid in two-dimensional, unsteady, incompressible flows is a much studied problem. Besides experimental and numerical studies, theoretical results are also available for certain classes of flows. These classes include time-periodic flows (see, e.g., [7,19,26–29,33,35]) and quasiperiodic flows (see, e.g., [4,5,8,33]), where the transport problem can be reformulated in terms of appropriately defined two-dimensional Poincaré maps. If these maps admit hyperbolic fixed points whose stable and unstable manifolds intersect transversely, then the chaotic mixing of initial conditions between the interior and the exterior of the resulting homoclinic or heteroclinic tangle can be studied via lobe dynamics. The long term evolution of lobes (i.e., the "building blocks" of the tangle) can be traced using the topological approximation method of Rom-Kedar [26,27]. The idea of chaotic transport through lobes can be generalized to adiabatic flows (see [15,16]), almost periodic flows (see [20,30]), flows with infinite time hyperbolicity and bounded velocity [1], three-dimensional, incompressible flows (see [10,14,17,18,21], and general, higher-dimensional Hamiltonian systems (see [2,3,32]).

While these results provide very efficient tools for the study of flows with special time-dependence or special structure, their application becomes difficult or impossible in the case of general fluid flows given in terms of experimentally or numerically generated vector fields. First, "real-life" flows have general time-dependence and

★ This research was supported by ONR Grant No. N00014-93-I-0691.

* Corresponding author. E-mail: haller@cfm.brown.edu. Partially supported by NSF Grant No. DMS-95-01239 and an Alfred P. Sloan Fellowship.

PII S0167-2789(98)00091-8

hence their evolution cannot be captured through the iteration of Poincaré maps. More importantly, while the formation of infinitely many lobes is generic in periodic, quasiperiodic and almost periodic flows with intersecting stable and unstable manifolds, hyperbolic structures in aperiodic flows need not admit any lobes at all, which prevents the application of lobe dynamics. Second, existing analytic transport calculations are usually based on some version of the Melnikov method, which requires the presence of an infinitesimally small perturbation parameter in the flow. This means that the flow must be very close to an integrable, steady limit in all spatial domains and for all times. Such uniform near-integrability cannot be expected in most applications. Besides, there is no general strategy for extracting a uniformly small perturbation parameter from a given experimental or numerical data set. Third, all the above results assume that the flow admits a hyperbolic structure and lobes for all times. This assumption is very hard to satisfy, as hyperbolic structures in most real life flows are of transient nature. In summary, while the concept of mixing due to the interaction of stable and unstable manifolds is very useful in interpreting complicated data sets from fluid flows (see, e.g., [22,23,25]), the existing analytical tools for the description of Lagrangian transport cannot be applied to all such data sets.

In addition to the technical difficulties cited above, there is also a conceptual difficulty with the application of Lagrangian transport ideas to large-scale fluid motions, such as those in oceanography and atmospheric science. The fact is that most data sets provide *Eulerian information*, such as contour plots of a streamfunction, height field, temperature, salinity, i.e., a scalar quantity, while the *Lagrangian information*, and the existence of stable and unstable manifolds, tangles, and lobes, remains hidden. This necessitates further numerical treatment of the data (i.e., integration of a numerically generated vector field), which introduces additional errors in the study of the flows that are approximately known to begin with. For flows with long time scales, these errors coupled with the lack of special time-dependence make it virtually impossible to identify hyperbolic structures with the detail needed for existing mixing theories.

Our main goal in this paper is to develop tools for the study of Lagrangian mixing in general, aperiodic, two-dimensional Hamiltonian systems. We are interested in cases when the available Eulerian data, i.e., the time-dependent contour plot of the Hamiltonian, contains a saddle-type stagnation point on a finite time interval. Using Perron's method for the construction of invariant manifolds, we derive a set of three conditions involving Eulerian quantities under which the flow contains a solution with "finite-time hyperbolicity". Our conditions basically express the requirement that the speed of the Eulerian stagnation point and the attached Eulerian stable and unstable sets should be below a critical value over which Eulerian data and Lagrangian dynamics become uncorrelated. We note that for analytic examples with a small parameter ϵ, Theorem 3.1 can be used to estimate the maximal value of ϵ for which the flow admits a hyperbolic solution.

Next, we assume that the time-dependent, Eulerian stable and unstable sets of the stagnation point form a loop, which we consider a *kinematic eddy* (see, e.g., [34] for a similar definition of an eddy). For the finite time in question, we construct finite-time stable and unstable manifolds for the hyperbolic solution that can be used to define a *dynamic eddy* in the three-dimensional extended phase space. Solutions inside the dynamic eddy exhibit swirling, while solutions outside the eddy show translational motion. The invariant manifolds marking the boundary of the dynamic eddy are non-unique, but they are exponentially unique with respect to the lifetime of the eddy. This means, e.g., that two possible stable manifolds must be within a distance which is exponentially small in the time of existence of the stagnation point.

We consider the transport of fluid between the interior and the exterior of the dynamic eddy. In most cases, the invariant manifolds described above do not intersect (i.e., do not form lobes), which means that the eddy continuously emits or absorbs initial conditions. In some cases a finite number of lobes is formed by the intersecting manifolds, which means that the flux into the eddy changes its sign in time. In either case, we are able to estimate the flux in terms of Eulerian quantities associated with the streamline plots. We derive a bound for the error in our estimates in terms of Eulerian quantities. This error is small if the growth of the kinematic eddy is small.

We apply our theory to a kinematic eddy–jet interaction model due to Dutkiewitz and Paldor [9]. This analytic model has periodic time-dependence, but we restrict our study to the time of existence of the kinematic eddy within one period, hence periodicity is not used in our analysis. For physically relevant parameter configurations, we use the Eulerian streamline plots to show that our conditions for the existence of finite-time hyperbolicity in the flow are satisfied. We construct a solution with transient hyperbolicity numerically to illustrate our main result. We also show the non-existence of hyperbolicity in the flow in some cases when our basic conditions are not satisfied. Finally, we study the finite-time transport between the eddy and the jet, and demonstrate the accuracy of our Eulerian flux estimates by computing the actual Lagrangian flux numerically. We end the paper with some concluding remarks.

2. Hyperbolic stagnation points

Let us consider a two-dimensional, incompressible flow given by the velocity field:

$$\dot{x} = f_1(x, y, t) = \frac{\partial \psi(x, y, t)}{\partial y}, \qquad \dot{y} = f_2(x, y, t) = -\frac{\partial \psi(x, y, t)}{\partial x}. \tag{1}$$

Here the streamfunction ψ plays the role of a Hamiltonian and is assumed to be smooth in all its arguments. The level curves of ψ can be used to define coherent structures in the flow. For instance, a set of closed level curves bounded by a separatrix defines a "kinematic eddy", and a set of open level curves can be thought of as a jet.

Assume that for any fixed $t \in [t^-, t^+]$, the contour plot of $\psi(x, y, t)$ contains a hyperbolic (i.e., saddle–type) stagnation point

$$u(t) = (u_1(t), u_2(t)),$$

as shown in Fig. 1. For later convenience we assume that $t^-, t^+ > 0$. Our assumption implies that

$$\nabla\psi(u(t), t) = 0, \qquad \det[D^2\psi(u(t), t)] < 0, \tag{2}$$

where $D^2\psi$ denotes the Hessian matrix of second spatial derivatives of ψ. The second equation expresses the hyperbolicity of the stagnation point and immediately implies that the function $u(t)$ is smooth by the implicit function theorem. This enables us to estimate the magnitude of the speed of the stagnation point as $|\dot{u}(t)| \leq \mu$, where

$$\mu = \max_{t\in[t^-,t^+]} |[D^2\psi]^{-1}\nabla(\partial_t\psi)|_{(x,y)=u(t)}. \tag{3}$$

We note that the hyperbolicity of the stagnation point implies that for any fixed $t_0 \in [t^-, t^+]$, the phase portrait of the velocity field $f(x, y, t_0)$ contains a saddle point with one-dimensional stable and unstable subspaces. Considering the union of these lines for all $t \in [t^-, t^+]$, we obtain two, two-dimensional surfaces $S(u)$ and $U(u)$, respectively, which are attached to the curve $u(t)$ in the space of the variables (x, y, t). We will refer to $S(u)$ and $U(u)$ as *Eulerian stable and unstable bundles*, respectively (see Fig. 2).

We are interested in finding conditions under which the Eulerian observation of the saddle-type stagnation curve $u(t)$ implies the presence of an actual saddle-type particle path in the extended of (x, y, t) phase space of Eq. (1). In general, one expects such a relationship only if the motion of the stagnation point is not too fast compared to typical particle velocities, i.e., the discrepancy between streamlines and particle paths develops on relatively long time scales near $u(t)$. Such long (but finite) time scales are typical in oceanographic and atmospheric problems.

We first pass to the moving frame of the stagnation point by introducing the change of coordinates

$$z = (x, y) - u(t),$$

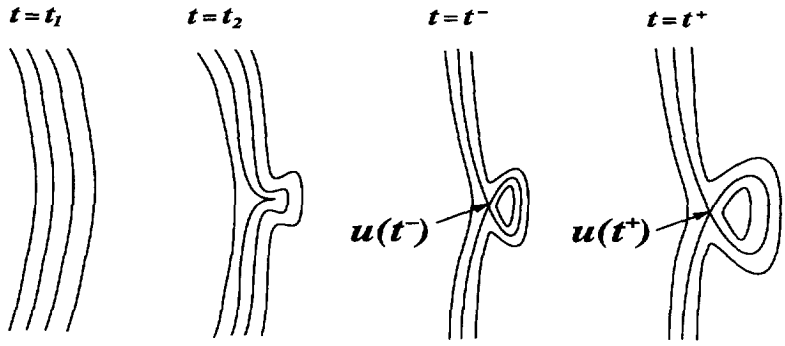

Fig. 1. Transient hyperbolic stagnation point.

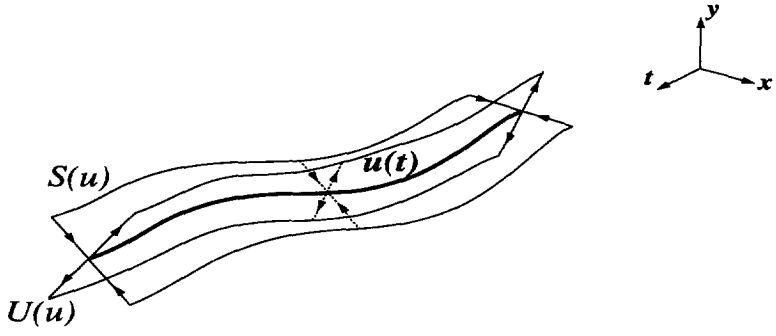

Fig. 2. Eulerian stable and unstable bundles.

which transforms Eq. (1) to

$$\dot{z} = \nabla f(u(t), t)z + F(z, t) - \dot{u}(t) \tag{4}$$

with

$$F(z, t) = f(z + u(t), t) - \nabla f(u(t), t)z = \mathrm{O}(|z|^2).$$

The smoothness of F implies the estimate

$$|F(z, t)| < C_F|z|^2 \tag{5}$$

for $t \in [t^-, t^+]$ and $|z| \leq C_z$, where

$$C_F = \max_{t\in[t^-,t^+]} \max_{|z|\leq C_z} \tfrac{1}{2}||D^2 f(z + u(t), t)||. \tag{6}$$

Furthermore, for all $|z|, |\bar{z}| \leq C_z$ and $t \in [t^-, t^+]$, we have

$$|F(z, t) - F(\bar{z}, t)| \leq L_F|z - \bar{z}|,$$

where

$$L_F = \sum_{i=1}^{2} \max_{t\in[t^-,t^+]} \max_{|z|\leq C_z} |\nabla f_i(z + u(t), t) - \nabla f_i u(t), t)|. \tag{7}$$

By the hyperbolicity of the stagnation point, the matrix $\nabla(fu(t), t)$ admits two eigenvalues $\lambda(t) > 0$ and $-\lambda(t) < 0$, which are both smooth functions of time. We introduce the notation

$$\lambda_{\max} = \max_{t\in[t^-,t^+]} \lambda(t), \qquad \lambda_{\min} = \min_{t\in[t^-,t^+]} \lambda(t), \qquad \lambda'_{\max} \equiv \max_{t\in[t^-,t^+]} |\dot{\lambda}(t)|.$$

We also introduce the matrix $T(t) \in \mathbb{R}^{2\times 2}$ with $\det T(t) = 1$, whose columns are the eigenvectors corresponding to $-\lambda(t)$ and $\lambda(t)$, respectively. We will use the constants

$$C_T = \max_{t\in[t^-,t^+]} ||T(t)||, \qquad C'_T = \max_{t\in[t^-,t^+]} \left\| \frac{\mathrm{d}}{\mathrm{d}t} T(t) \right\|. \tag{8}$$

The change of variables

$$w = T^{-1}(t)z$$

puts Eq. (4) to the form

$$\dot{w} = \Lambda(t)w + M(w,t) + N(w,t), \tag{9}$$

where

$$\Lambda(t) = \mathrm{diag}(-\lambda(t), \lambda(t)), \quad M(w,t) = T^{-1}(t)F(T(t)w,t), \quad N(w,t) = -T^{-1}(t)\left[\frac{\mathrm{d}T(t)}{\mathrm{d}t}w + \dot{u}(t)\right]. \tag{10}$$

The following estimates hold:

$$|M(w,t)| \le C_T^3 C_F |w|^2, \qquad |N(w,t)| \le C_T[C'_T|w| + \mu], \tag{11}$$

where we used formulas (3), (5), and (8). Formulas (7) and (10) also give the following Lipschitz constants for the functions M and N:

$$L_M = C_T^2 L_F, \qquad L_N = C_T C'_T. \tag{12}$$

Note that without the terms M and N, $w = 0$ is a solution of (9) for $t \in [t^-, t^+]$. This solution also admits stable and unstable subspaces given by $w_2 = 0$ and $w_1 = 0$, respectively.

3. Invariant manifolds

In this section we study the survival of invariant structures near $w = 0$ in Eq. (9) after we add the terms M and N. In particular, we want to construct a one-dimensional, normally hyperbolic invariant manifold with stable and unstable manifolds for Eq. (9). The manifolds we construct will differ from those commonly used in the geometric theory of dynamical systems (see, e.g., [11]) because of the finite time of existence of the stagnation point.

3.1. The derivation of the integral equation

We fix a small number $\delta > 0$ and select a C^∞ bump function b_1 with the properties

$$b_1(s) = \begin{cases} 1 & \text{if } s \le C_T C_z(1-\delta)/\sqrt{2}, \\ 0 & \text{if } s \ge C_T C_z/\sqrt{2}, \end{cases}$$

and with $0 < b_1(s) < 1$ for $s \in (C_T C_z(1-\delta)/\sqrt{2}, C_T C_z/\sqrt{2})$. We also need author C^∞ bump function b_2 with the properties

$$b_2(s) = \begin{cases} 1 & \text{if } t^-(1+\delta) \le s \le t^+(1-\delta), \\ 0 & \text{if } s \le t^- \text{ or } s \ge t^+, \end{cases}$$

and with $0 < b_1(s) < 1$ for $s \in (t^-, t^-(1+\delta)) \cup (t^+(1-\delta), t^+)$. We use these functions to smoothly modify the vector field (9), so that for $|w_i| \ge C_T C_z/\sqrt{2}$ and for $t \notin [t^-, t^+]$, it coincides with the vector field $\dot{w} = \Lambda(t)w$. We first extend the definition of M and N for all times by letting

$$M(w,t) = N(w,t) \equiv 0, \quad t \notin [t^-, t^+].$$

We then extend the definition of $\Lambda(t) = \mathrm{diag}(-\lambda(t), \lambda(t))$ for all times in a C^∞ fashion such that

$$\lambda(t) \in [\lambda_{\min}, \lambda_{\max}], \qquad |\dot{\lambda}(t)| \le \lambda'_{\max} \tag{13}$$

for all $t \in [t^-, t^+]$. Then the modified vector field

$$\dot{w} = \Lambda(t)w + \tilde{M}(w,t) + \tilde{N}(w,t), \tag{14}$$

with

$$\tilde{M}(w,t) = b_1(|w_1|)b_1(|w_2|)b_2(t)M(w,t), \qquad \tilde{N}(w,t) = b_1(|w_1|)b_1(|w_2|)b_2(t)N(w,t),$$

is smooth for all $w \in \mathbb{R}^2$ and $t \in \mathbb{R}$. Eq. (14) coincides with Eq. (9) for $|w_i| \le (1-\delta)C_T C_z/\sqrt{2}$ and $t \in [t^-(1+\delta), t^+(1-\delta)]$. Furthermore, our estimates (11), the definition of b_i, and the extension (13) imply the global estimates

$$\begin{aligned} &\lambda_{\min} \le \lambda(t) \le \lambda_{\max}, \qquad |\dot{\lambda}(t)| \le \lambda'_{\max}, \\ &|\tilde{M}(w,t)| \le C_T^3 C_F C_z |w|, \qquad |\tilde{N}(w,t)| \le C_T[\mu + C'_T|w|]. \end{aligned} \tag{15}$$

Introducing the notation

$$w = (w_s, w_u), \qquad \tilde{M} = (\tilde{M}_s, \tilde{M}_u), \qquad \tilde{N} = (\tilde{N}_s, \tilde{N}_u),$$

then dropping the tildes, we can rewrite Eq. (14) as an integral equation of the form

$$\begin{aligned} w_s(t) &= \mathrm{e}^{-\int_{t_s}^t \lambda(\tau)\,\mathrm{d}\tau} w_s(t_s) + \int_{t_s}^t \mathrm{e}^{-\int_\tau^t \lambda(s)\,\mathrm{d}s}[M_s(w(\tau),\tau) + N_s(w(\tau),\tau]\,\mathrm{d}\tau, \\ w_u(t) &= \mathrm{e}^{\int_{t_u}^t \lambda(\tau)\,\mathrm{d}\tau} w_u(t_u) + \int_{t_u}^t \mathrm{e}^{\int_\tau^t \lambda(s)\,\mathrm{d}s}[M_u(w(\tau),\tau) + N_u(w(\tau),\tau)]\,\mathrm{d}\tau. \end{aligned} \tag{16}$$

We fix a number q with $0 < q < 1$, and define the stable manifold W^s as

$$W^s = \left\{ w^0 \,|\, \sup_{t \ge 0}[|w(t; w^0)|\mathrm{e}^{-q\int_0^t \lambda(\tau)\,\mathrm{d}\tau}] < \infty \right\}.$$

In other words, W^s contains the set of initial conditions which never leave the box $|w_i| = C_T C_z/\sqrt{2}$ in forward time. (If they left this box, they would grow as $\exp(\int_0^t \lambda(\tau)\,\mathrm{d}\tau)$, and hence the supremum in the definition of W^s

would not be bounded.) Note that W^s is a positively invariant set by definition, and for any solution $w(t) \in W^s$ and for any fixed $t \in \mathbb{R}$, we have

$$\lim_{t_u\to\infty} |e^{\int_{t_u}^{t}\lambda(\tau)\,d\tau} w_u(t_u)| \le \lim_{t_u\to\infty} e^{\int_{t_u}^{t}\lambda(\tau)d\tau} K e^{q\int_0^{t_u}\lambda(\tau)\,d\tau} < \lim_{t_u\to\infty} K e^{\lambda_{\max}(t-t_u)} e^{q\lambda_{\max}t_u} = 0.$$

Therefore, taking the limit $t_u \to \infty$ in Eq. (16), setting $t_s = 0$ and $w_s(t_s) = w_s$, we obtain that solutions in W^s satisfy the integral equation

$$\begin{aligned} w_s(t) &= e^{-\int_0^t \lambda(\tau)\,d\tau} w_s + \int_0^t e^{-\int_\tau^t \lambda(s)\,ds}[M_s(w(\tau),\tau) + N_s(w(\tau),\tau)]\,d\tau, \\ w_u(t) &= \int_\infty^t e^{\int_\tau^t \lambda(s)\,ds}[M_u(w(\tau),\tau) + N_u(w(\tau),\tau)]\,d\tau. \end{aligned} \tag{17}$$

We will show that W^s is a non-empty set by proving that this integral equation has a unique solution $w(t)$ with $w_s(0) = w_s$.

3.2. The contraction mapping argument

We can recast the integral Eq. (17) in the form

$$w(t) = \mathcal{F}(w(t)),$$

which shows that a solution of (17) is a fixed point of the map $\mathcal{F}$. Let us introduce the weighted norm

$$||w||_q = \sup_{t\ge 0} e^{-q\int_0^t \lambda(\tau)\,d\tau} ||w(t)||,$$

with some $0 \le q < 1$. We also define the function space

$$B_{q,K} = \{w(t)\colon [0,\infty] \to \mathbb{R}^2 \mid w \in C^0[0,\infty),\ ||w||_q \le K\}.$$

It is easy to see that $B_{q,K}$ is a complete metric space in the norm $\|\cdot\|_q$. We want to show that $\mathcal{F}$ is a contraction mapping on this space. We will make use of the estimate

$$\int_a^b |e^{p\int_r^t \lambda(s)\,ds}|\,d\tau \le \frac{|p|\lambda_{\min}}{|p|\lambda_{\min}^2 - \lambda'_{\max}} |e^{p\int_b^t \lambda(s)\,ds} - e^{p\int_a^t \lambda(s)\,ds}| \tag{18}$$

for any $a < b$ and $p \in \mathbb{R}$ with $|p|\lambda_{\min}^2 - \lambda'_{\max} > 0$. This estimate follows easily after integration by parts.

First we have to show that $\mathcal{F}(B_{q,K}) \subset B_{q,K}$. From the integral Eq. (17) we obtain the estimate

$$\begin{aligned} \|\mathcal{F}(w(t))\| \le{}& e^{-\int_0^t \lambda(\tau)\,d\tau}|w_s| + \int_0^t e^{-\int_\tau^t \lambda(s)\,ds}[|M_s(w(\tau),\tau)| + |N_s(w(\tau),\tau)|]\,d\tau \\ &+ \int_t^\infty e^{\int_\tau^t \lambda(s)\,ds}[|M_u(w(\tau),\tau)| + |N_u(w(\tau),\tau)|]\,d\tau \end{aligned}$$

$$< e^{-\int_0^t \lambda(\tau)\,d\tau} C_T C_z/\sqrt{2} + \int_0^t e^{-\int_\tau^t \lambda(s)\,ds}[C_T^3 C_F C_z|w| + C_T[C_T'|w| + \mu]]\,d\tau$$

$$+ \int_t^\infty e^{\int_\tau^t \lambda(s)\,ds}[C_T^3 C_F C_z|w| + C_T[C_T'|w| + \mu]]\,d\tau. \tag{19}$$

Multiplying by $\exp[-q\int_0^t \lambda(s)\,ds]$, taking the supremum of both sides in t, and using $\|w\|_q \le K$ along with the estimate (18) gives

$$\|\mathcal{F}(w(t))\|_q \le C_T C_z/\sqrt{2} + \frac{2C_T\lambda_{\min}[K(C_T^2 C_F C_z + C_T') + \mu][(1-q^2) - \lambda_{\min}^2 - \lambda_{\max}']}{[(1-q)\lambda_{\min}^2 - \lambda_{\max}'][(1+q)\lambda_{\min}^2 - \lambda_{\max}']},$$

where we assumed that

$$(1-q)\lambda_{\min}^2 > \lambda_{\max}'. \tag{20}$$

Therefore, $\|\mathcal{F}(w(t))\|_q \le K$ and hence $\mathcal{F}(w(t)) \in B_{q,K}$ will hold for K sufficiently large provided

$$\frac{2C_T\lambda_{\min}(C_T^2 C_F C_z + C_T')[(1-q^2) - \lambda_{\min}^2 - \lambda_{\max}']}{[(1-q)\lambda_{\min}^2 - \lambda_{\max}'][(1+q)\lambda_{\min}^2 - \lambda_{\max}']} < 1. \tag{21}$$

Next we have to argue that $\mathcal{F}$ is a contraction mapping on the space $B_{q,K}$. For any two functions $w, \bar{w} \in B_{q,K}$ with $w_s(0) = \bar{w}_s(0)$, the integral Eq. (17) holds, and an estimate similar to (19) leads to

$$\|\mathcal{F}(w(t)) - \mathcal{F}(\bar{w}(t))\|_q \le \frac{2C_T\lambda_{\min}(C_T L_F + C_T')[(1-q^2)\lambda_{\min}^2 - \lambda_{\max}']}{[(1-q)\lambda_{\min}^2 - \lambda_{\max}'][(1+q)\lambda_{\min}^2 - \lambda_{\max}']}\|w(t) - \bar{w}(t)\|_q.$$

This inequality shows that $\mathcal{F}$ is a contraction mapping whenever

$$\frac{2C_T\lambda_{\min}(C_T L_F + C_T')[(1-q^2)\lambda_{\min}^2 - \lambda_{\max}']}{[(1-q)\lambda_{\min}^2 - \lambda_{\max}'][(1+q)\lambda_{\min}^2 - \lambda_{\max}']} < 1. \tag{22}$$

As a result, Eq. (17) has a unique solution for any $w_s(0) = w_s$. The derivative of the solution with respect to w_s obeys the same estimates, hence we obtain that the solution of (17) is a C^1 function of w^s, i.e., the set W^s is a C^1 manifold. A similar argument establishes the existence of C^1 manifold of solutions W^u defined as

$$W^u = \left\{ w^0 \,|\, \sup_{t\le 0}[|w(t; w^0)|e^{-q\int_0^t \lambda(\tau)\,d\tau}] < \infty \right\}.$$

Both W^u and W^s are C^1-close to the stable and unstable subspaces of the equation $\dot{w} = A(t)w$, therefore they must intersect transversely in a one-dimensional curve Γ which is C^1-close to the curve $w = 0, t \in \mathbb{R}$ in the extended phase space of the (x, y, t) variables. The curve Γ admits local stable and unstable manifolds, and we have

$$W_{\text{loc}}^s(\Gamma) \equiv W^s, \qquad W_{\text{loc}}^u(\Gamma) \equiv W^u.$$

Note that for $t \notin [t^-, t^+]$, $\Gamma(t) \equiv 0$ holds since Γ must coincide with the trivial solution of the equation $\dot{w} = \tilde{A}(t)w$ (see Fig. 3). By the continuity of $\Gamma(t)$, this implies that $\Gamma(t)$ is globally bounded and hence we can select $q = 0$ in all our previous estimates.

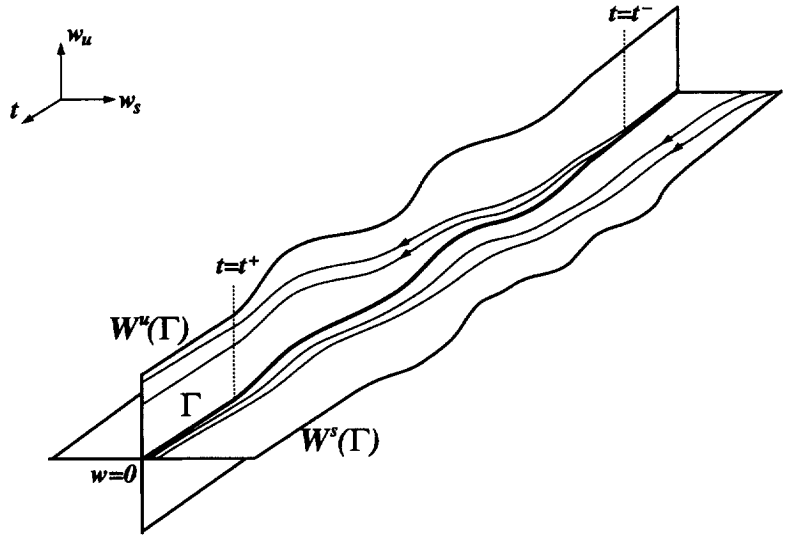

Fig. 3. Local invariant manifolds for the bumped vector field.

3.3. The size estimate

We have to make sure that the invariant manifolds found above also exist for the original, unmodified Eq. (9) as locally invariant manifolds. Although they are C^1-close to the curve $u(t)$, their C^0 distance from $u(t)$ may be such that they leave the box in which the modified system is related to (9). To avoid this, we have to ensure that the solution $\Gamma(t)$ on the curve Γ obeys the estimates $|\Gamma_i(t)| \leq (1-\delta)C_T C_z/\sqrt{2}$ for $t \in [t^-, t^+]$.

Since $\Gamma(t)$ lies in the intersection of W^s and W^u, it solves the integral Eq. (17), which yields the following expression for $\Gamma(t)$:

$$\begin{aligned}\Gamma_s(t) &= \int_0^t e^{-\int_\tau^t \lambda(s)\,ds}[M_s(\Gamma(\tau),\tau) + N_s(\Gamma(\tau),\tau)]\,d\tau,\\ \Gamma_u(t) &= \int_\infty^t e^{-\int_\tau^t \lambda(s)\,ds}[M_u(\Gamma(\tau),\tau) + N_u(\Gamma(\tau),\tau)]\,d\tau.\end{aligned} \tag{23}$$

Let us fix a constant time $\bar{t} > 0$ and let

$$\bar{\Gamma} = \sup_{t\in[0,\bar{t}]} |\Gamma(t)|.$$

Then (23) together with (11) and (18) gives the estimate

$$\bar{\Gamma} \leq 2\frac{C_T\lambda_{\min}}{\lambda_{\min}^2 - \lambda'_{\max}}[C_T^2 C_F \bar{\Gamma} + C'_T\bar{\Gamma} + \mu],$$

which can be rewritten as

$$C_T^2 C_F \bar{\Gamma}^2 - \left[\frac{\lambda_{\min}^2 - \lambda'_{\max}}{2C_T\lambda_{\min}} - C'_T\right]\bar{\Gamma} + \mu \geq 0. \tag{24}$$

If

$$\mu < \frac{1}{4C_T^2 C_F}\left[\frac{\lambda_{\min}^2 - \lambda'_{\max}}{2C_T\lambda_{\min}} - C'_T\right]^2,$$

then inequality (24) is equivalent to

$$0 \le \bar{\Gamma} \le \Gamma_- \quad \text{or} \quad \bar{\Gamma} \ge \Gamma_+,$$

where $0 < \Gamma_- < \Gamma_+$ are the zeros of the right-hand-side of (24). These estimates are independent of the time t and $\bar{\Gamma}$ is a continuous function of $\bar{t}$, therefore $\bar{\Gamma} \le \Gamma_-$ must hold since for $\bar{t} = 0$ we have $\bar{\Gamma} = 0$. Hence $\Gamma(t)$ is a locally invariant curve for the original, unmodified system if $\Gamma_- \le (1-\delta)C_T C_z$. This holds for $\delta > 0$ small enough, provided $\Gamma_- \le C_T C_z$, i.e.,

$$\mu < \left[\frac{\lambda_{\min}^2 - \lambda'_{\max}}{2C_T\lambda_{\min}} - C'_T\right] C_T C_z - C_T^2 C_z^2 C_F. \tag{25}$$

3.4. The decay estimate

We now want to show that solutions that start close enough to $\Gamma(t)$ within the manifolds $W^s(\Gamma)$ and $W^u(\Gamma)$ approach $\Gamma(t)$ at an exponential rate in forward and backward time, respectively, as long as $t \in [t^-, t^+]$. We describe the argument for the stable manifold only, since the unstable manifold can be dealt with similarly.

Consider a solution $X(t) = (x(t), y(t)) \in W^s(\Gamma)$. Using the integral equations (17) and (23), we can write

$$\begin{aligned}|X(t) - \Gamma(t)| \le{}& e^{-\int_{t_0}^{t}\lambda(s)\,ds}|X(t_0) - \Gamma(t_0)| \\ &+ \int_{t_0}^{t} e^{-\int_{t_0}^{\tau}\lambda(s)\,ds}[C_T^3 C_F C_z + C_T C'_T]|X(\tau) - \Gamma(\tau)|\,d\tau \\ &+ \int_{\infty}^{t} e^{\int_{\infty}^{\tau}\lambda(s)\,ds}[C_T^3 C_F C_z + C_T C'_T]|X(\tau) - \Gamma(\tau)|\,d\tau.\end{aligned}$$

Introducing the quantity

$$\Delta(T) = \sup_{t\in[t_0,T]} |X(t) - \Gamma(t)| e^{\int_{t_0}^{t}\lambda(s)\,ds},$$

and combining the above estimate with (18) we obtain that

$$\Delta(T) \le \Delta(t_0) + \frac{2C_T[C_T^2 C_F C_z + C'_T]\lambda_{\min}}{\lambda_{\min}^2 - \lambda'_{\max}}\Delta(T).$$

If (22) holds with $q = 0$, then this last inequality implies

$$|X(t) - \Gamma(t)| \le \frac{(\lambda_{\max}^2 - \lambda'_{\max})|X(t_0) - \Gamma(t_0)|}{\lambda_{\min}^2 - \lambda'_{\max} - 2C_T[C_T^2 C_F C_z + C'_T]\lambda_{\min}} e^{-\int_{t_0}^{t}\lambda(s)\,ds}. \tag{26}$$

3.5. Non-uniqueness of invariant manifolds

It is important to note that the locally invariant manifolds we have constructed are *not* unique. The non-uniqueness comes from the fact that in our contraction mapping argument we modified the original vector field (1) outside the time interval $t \in [t^-, t^+]$, and this modification can be chosen in different ways. In this section we want to argue that if the time of existence for the stagnation point is long enough (i.e., $t^+ - t^-$ is a large number), then all possible "finite-time" stable and unstable manifolds are exponentially close to the "master" manifolds $W^{\mathrm{u}}(\Gamma)$ and $W^{\mathrm{s}}(T)$ near Γ. This fact also implies that Γ is uniquely determined up to exponentially small errors. The significance of this result is that Γ and its stable and unstable manifolds will appear to be unique in numerical simulations, if the time scale of interest is long enough.

We start by defining the *finite-time invariant manifolds*

$$W^{\mathrm{s}}_{\mathrm{loc}}(t^-, t^+) = \{(z(t), t) | |z(t; z_0) - \Gamma(t)| \leq |z(t^-; z_0) - \Gamma(t^-)|, t \in (t^-, t^+]\},$$
$$W^{\mathrm{u}}_{\mathrm{loc}}(t^-, t^+) = \{(z(t), t) | |z(t; z_0) - \Gamma(t)| \leq |z(t^+; z_0)|, -\Gamma(t^+)|, t \in [t^-, t^+)\}.$$

Note that the finite-time stable manifold $W^{\mathrm{s}}_{\mathrm{loc}}(t^-, t^+)$ contains solutions $z(t)$ whose distance from the solution $\Gamma(t)$ does not exceed the initial distance $|z(t^-; z_0) - \Gamma(t^-)|$ for times $t \in [t^-, t^+]$. Similarly, the finite-time unstable manifold $W^{\mathrm{u}}_{\mathrm{loc}}(t^-, t^+)$ is the set of solutions whose distance from $\Gamma(t)$ does not exceed the final distance $|z(t^+; z_0) - \Gamma(t^+)|$. The definition of these finite-time manifolds is motivated by how one would try to locate possible stable and unstable manifolds numerically in a finite-time data set. By the smoothness of the flow with respect to the initial conditions, both of the above sets are closed and their boundaries are piecewise smooth. Furthermore, both $W^{\mathrm{s}}_{\mathrm{loc}}(t^-, t^+)$ and $W^{\mathrm{u}}_{\mathrm{loc}}(t^-, t^+)$ have non-zero volume in the (x, y, t).

The master stable manifold $W^{\mathrm{s}}(\Gamma)$ near Γ is given by a function $w_{\mathrm{u}} = g_{\mathrm{u}}(w_{\mathrm{s}}, t)$. Introducing the new coordinate

$$v_{\mathrm{u}} = w_{\mathrm{u}} - g_{\mathrm{u}}(w_{\mathrm{s}}, t),$$

we obtain the equation

$$\dot{v}_{\mathrm{u}} = \dot{w}_{\mathrm{u}} - \partial_{w_{\mathrm{s}}} g_{\mathrm{u}} \dot{w}_{\mathrm{s}} - \partial_t g_{\mathrm{u}} = \lambda v_{\mathrm{u}} + \lambda g_{\mathrm{u}} - \partial_{w_{\mathrm{s}}} g_{\mathrm{u}}(-\lambda w_{\mathrm{s}} + M_{\mathrm{s}} + N_{\mathrm{s}}) - \partial_t g_{\mathrm{u}}.$$

The local invariance condition $\dot{v}_{\mathrm{u}}|_{v_u=0} = 0$ implies that the above equation can be rewritten as

$$\dot{v}_{\mathrm{u}} = [\lambda(t) + G_{\mathrm{u}}(w_{\mathrm{s}}, v_{\mathrm{u}}, t)]v_{\mathrm{u}}, \tag{27}$$

where the function G_{u} is of order $\mathrm{O}(\mu, C_z)$. Then (27) implies the estimate

$$|v_{\mathrm{u}}(t)| \geq |v_{\mathrm{u}}(t^-)| \mathrm{e}^{\int_{t^-}^{t} \lambda(\tau) - \mathrm{O}(\mu, C_z)\, \mathrm{d}\tau}. \tag{28}$$

This inequality gives that $v_{\mathrm{u}}(t^+) > C_T C_z$ holds if

$$|v_{\mathrm{u}}(t^-)| > C_T C_z \exp\left[-\int_{t^-}^{t^+} [\lambda(\tau) - \mathrm{O}(\mu, C_z)]\, \mathrm{d}\tau \right].$$

Therefore, any point $z \in W^{\mathrm{s}}_{\mathrm{loc}}(t^-, t^+)$ must necessarily satisfy the estimate

$$\mathrm{dist}(z, W^{\mathrm{s}}_{\mathrm{loc}}(\Gamma)) < C_T C_z \mathrm{e}^{-\int_{t^-}^{t^+} [\lambda(\tau) - \mathrm{O}(\mu, C_z)]\, \mathrm{d}\tau}.$$

A similar argument yields that points in $W^{\mathrm{u}}_{\mathrm{loc}}(t^-, t^+)$ are exponentially close to the master unstable manifold $W^{\mathrm{u}}_{\mathrm{loc}}(\Gamma)$.

Let us assume now that there exists a two-dimensional invariant manifold $\hat{W}^{\mathrm{s}}_{\mathrm{loc}} \neq W^{\mathrm{u}}_{\mathrm{loc}}(\Gamma)$ and $\hat{K} > 0$ such that any solution $X(t) \in \hat{W}^{\mathrm{s}}_{\mathrm{loc}}$, $t \in [t^-, t^+]$ satisfies the decay estimate

$$|X(t) - \Gamma(t)| \leq \hat{K} \mathrm{e}^{-\int_{t_-}^{t} \lambda(s)\,\mathrm{d}s}.$$

Then inequality (28) implies that for this solution we have

$$|v_{\mathrm{u}}(t^-)| \leq \hat{K} \mathrm{e}^{-\int_{t^-}^{t'} 2\lambda(s) - \mathrm{O}(\mu, C_z)\,\mathrm{d}s}.$$

In summary, other two-dimensional, locally invariant, unstable manifolds asymptotic to hyperbolic solutions will in general coexist with the master manifolds we constructed, but will be exponentially close to Γ, $W^{\mathrm{s}}_{\mathrm{loc}}(\Gamma)$, and $W^{\mathrm{u}}_{\mathrm{loc}}(\Gamma)$, respectively.

3.6. The main theorem

Here we collect all the conditions that are needed for the existence of the normally hyperbolic solution $\Gamma(t)$ for $t \in [t_-, t_+]$:

$$\begin{aligned}
&\lambda^2_{\min} > \lambda'_{\max},\\
&\lambda^2_{\min} > \lambda'_{\max} + 2C_T\lambda_{\min}(C_T^2 C_F C_z + C'_T),\\
&\lambda^2_{\min} > \lambda'_{\max} + 2C_T\lambda_{\min}(C_T^2 L_F + C'_T),\\
&\mu < \frac{1}{4C_T^2 C_F}\left[\frac{\lambda^2_{\min} - \lambda'_{\max}}{2C_T\lambda_{\min}} - C'_T\right]^2,\\
&\mu < \left[\frac{\lambda^2_{\min} - \lambda'_{\max}}{2C_T\lambda_{\min}} - C'_T\right] C_T C_z - C_T^4 C_z^2 C_F.
\end{aligned} \tag{29}$$

If we define

$$\bar{C} = \max(C_F C_z, L_F), \tag{30}$$

then the inequalities in (29) simplify to

$$\begin{aligned}
&C'_T < \frac{\lambda^2_{\min} - \lambda'_{\max}}{2C_T\lambda_{\min}} - C_T^2\bar{C},\\
&\mu < \frac{1}{4C_T^2 C_F}\left[\frac{\lambda^2_{\min} - \lambda'_{\max}}{2C_T\lambda_{\min}} - C'_T\right]^2,\\
&\mu < C_T C_z\left[\left[\frac{\lambda^2_{\min} - \lambda'_{\max}}{2C_T\lambda_{\min}} - C'_T\right] - C_T^3 C_F C_z\right].
\end{aligned} \tag{31}$$

We summarize our result in the following theorem:

Theorem 3.1. Suppose that conditions (31) are satisfied for system (1). Then, there exists a solution $\Gamma(t)$ with the following properties:

(i) For $t \in [t^-, t^+]$,

$$|\Gamma(t) - u(t)| < \frac{1}{2C_T^2 C_F}\left[\left[\frac{\lambda_{\min}^2 - \lambda'_{\max}}{2C_T\lambda_{\min}} - C'_T\right] - \sqrt{\left[\frac{\lambda_{\min}^2 - \lambda'_{\max}}{2C_T\lambda_{\min}} - C'_T\right]^2 - \mu}\right]$$
$$= \frac{\mu C_T \lambda_{\min}}{\lambda_{\min}^2 - \lambda'_{\max} - 2C_T C'_T \lambda_{\min}} + O(\mu^2).$$

(ii) $|\dot{\Gamma}(t) - \dot{u}(t)| \leq O(\mu)$.

(iii) The solution $\Gamma(t)$ has two-dimensional, locally invariant stable and unstable manifolds, $W^s(\Gamma)$ and $W^u(\Gamma)$, which are locally C^1 close to the Eulerian stable and unstable bundles $S(u)$ and $U(u)$ in the extended phase space (x, y, t).

(iv) There exists a constant $C > 1$ such that for any two solutions $\xi(t) \in W^s(\Gamma)$ and $\zeta(t) \in W^u(\Gamma)$, and for any time $t \in [t^-, t^+]$, with

$$|\xi(t_-) - \Gamma(t_-)| \leq C_z, \quad |\zeta(t_+) - \Gamma(t_+)| \leq C_z$$

we have

$$|\Gamma(t) - \xi(t)| \leq Ce^{-\int_{t_-}^{t} \lambda(\tau)\,d\tau}|\Gamma(t^-) - \xi(t^-)|, \qquad |\Gamma(t) - \zeta(t)| \leq Ce^{\int_{t^+}^{t} \lambda(\tau)\,d\tau}|\Gamma(t^+) - \zeta(t^+)|.$$

(v) If two manifolds $\hat{W}^u_{\text{loc}}(\Gamma)$ and $W^s_{\text{loc}}(\Gamma)$ also satisfy the properties listed in statements (i)–(iv), then

$$\text{dist}(\hat{W}^s_{\text{loc}} W^s_{\text{loc}}(\Gamma)), \text{dist}(\hat{W}^u_{\text{loc}}, W^u_{\text{loc}}(\Gamma)) < Ce^{\int_{t^-}^{t^+}[2\lambda(\tau) - O(\mu, C_z)]\,d\tau},$$

as shown in Fig. 4.

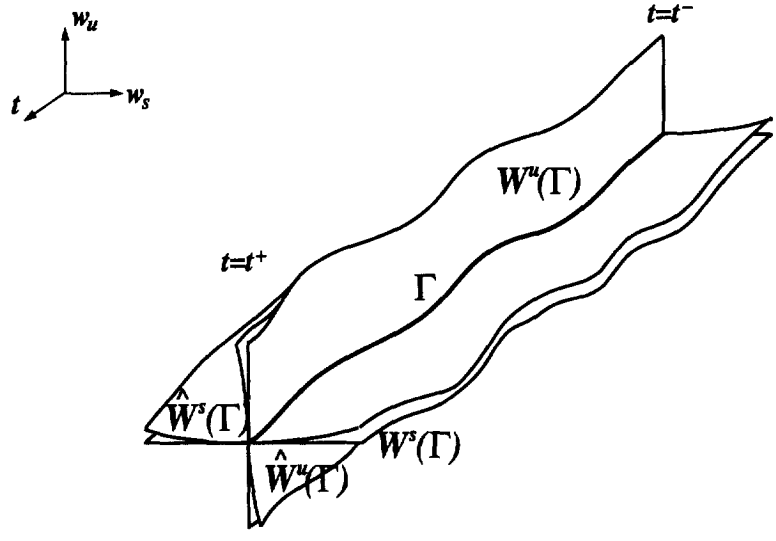

Fig. 4. Non-uniqueness of the invariant manifolds.

4. Kinematic and dynamic eddies

In this section we assume that the instantaneous stagnation points studied in Section 3 are contained in a closed level curve of the streamfunction. This means that the equilibrium point $u(t_0)$ of the vector field $f(x, y, t_0)$ has at least one homoclinic or heteroclinic loop ϕ_{t_0} attached to it. We assume for simplicity that ϕ_{t_0} is homoclinic, which indicates the presence of a *kinematic eddy* in the flow for $t \in [t^-, t^+]$. The $t = t_0$ slices of the two-dimensional surface

$$\Phi = \{(x, y, t_0) | (x, y) \in \phi_{t_0},\ t_0 \in [t^-, t^+]\}$$

serve as instantaneous boundaries for the kinematic eddy. For this reason, we refer to the two-dimensional homoclinic set Φ as the *kinematic eddy boundary.*

The global geometry of the stable and unstable manifolds of the solution Γ can be quite complicated or rather simple. We are interested in cases when they separate a bounded set from the rest of the phase space. In this bounded set we see swirling motion, whereas outside the bounded set the basic nature of motion is translational. We will call such a bounded set a *dynamic eddy*, and will define its boundary as the union of pieces of $W^s(\Gamma)$ and $W^u(\Gamma)$ with a "gate" surface through which initial conditions are exchanged (see Section 5 for a precise definition). We emphasize that we leave out vorticity consideration from our definitions of kinematic and dynamic eddies: kinematic eddies are objects identified from purely Eulerian observations, while dynamic eddies are directly linked with the actual Lagrangian dynamics of particles.

We are interested in locating dynamic eddies based on the Eulerian observation of kinematic eddies. In particular, we want to see how well the eddy boundary Φ approximates pieces of the locally invariant manifolds $W^u(\Gamma)$ and $W^s(\Gamma)$. To this end, we first estimate the distance of these manifolds and the eddy boundary within the C_z-neighborhood of the stagnation point, then use the solutions of system (1) to "propagate" our distance estimate outside this neighborhood.

In the local coordinates (w_s, w_u) used in the previous section, Φ can be written as

$$w_s = h_s(w_u; t_0), \qquad w_u = h_u(w_s; t_0)$$

with $h_s(0; t_0) = h_u(0; t_0) = h_s'(0; t_0) = h_u'(0; t_0) = 0$. (Here the prime refers to differentiation with respect to the first argument.) This just expresses the fact that the eddy boundary is tangent to the Eulerian stable and unstable bundles $S(u)$ and $U(u)$ of the curve $u(t)$. We now introduce the change of coordinates

$$\zeta_u = w_u - h_u(w_s; t), \qquad \zeta_s = w_s - h_s(w_u; t),$$

which "straightens out" the pieces of the kinematic eddy boundary that fall in the C_z-neighborhood of the stagnation curve $u(t)$. In particular, the "incoming" piece of the eddy boundary Φ is locally given by $\zeta_u \equiv 0$, while the "outgoing" piece of Φ locally satisfies $\zeta_s \equiv 0$. From Eq. (1) we obtain that

$$\begin{aligned}
\dot{\zeta}_s &= -\lambda(t)\zeta_s - \lambda(t)h_s(w_u; t) + M_s(w, t) + N_s(w, t), \\
&\quad - h_s'(w_u; t)[\lambda w_u + M_u(w, t) + N_u(w, t)] - \partial_t h_s(w_u; t), \\
\dot{\zeta}_u &= \lambda(t)\zeta_u + \lambda(t)h_u(w_s; t) + M_u(w, t) + N_u(w, t), \\
&\quad - h_s'(w_s; t)[-\lambda w_s + M_s(w, t) + N_s(w, t)] - \partial_t h_u(w_s; t),
\end{aligned}$$

Using the fact that kinematic eddy boundary is locally flat in the new coordinates, we can rewrite the above equation as

$$\dot{\zeta} = [\Lambda(t) + A(\zeta, t)]\zeta + B(\zeta, t), \tag{32}$$

with

$$A(\zeta,t)=\begin{pmatrix} a_{\mathrm{s}}(\zeta,t) & 0 \\ 0 & a_{\mathrm{u}}(\zeta,t)\end{pmatrix}, \qquad B(\zeta,t)=\begin{pmatrix} B_{\mathrm{s}}(\zeta,t) \\ B_{\mathrm{u}}(\zeta,t)\end{pmatrix}.$$

Here the components of A and B obey the estimates

$$|a_{\mathrm{s}}|\le C_A^{\mathrm{s}}, \quad |a_{\mathrm{u}}|\le C_A^{\mathrm{u}}, \quad |B_{\mathrm{s}}|\le C_B^{\mathrm{s}}, \quad |B_{\mathrm{u}}|\le C_B^{\mathrm{u}},$$

with the constants defined as

$$\begin{aligned} C_A^{\mathrm{s}} &\equiv \max_{t\in[t^-,t^+]}\max_{|w|\le C_T C_z} |\partial_{w_{\mathrm{u}}} M_{\mathrm{u}} - h_{\mathrm{u}}'\partial_{w_{\mathrm{u}}} M_{\mathrm{s}}|,\\ C_A^{\mathrm{u}} &\equiv \max_{t\in[t^-,t^+]}\max_{|w|\le C_T C_z} |\partial_{w_{\mathrm{s}}} M_{\mathrm{s}} - h_{\mathrm{s}}'\partial_{w_{\mathrm{s}}} M_{\mathrm{u}}|,\\ C_B^{\mathrm{s}} &\equiv \max_{t\in[t^-,t^+]}\max_{|w|\le C_T C_z} |N_{\mathrm{s}} - h_{\mathrm{s}}' N_{\mathrm{u}} - \partial_t h_{\mathrm{s}}|,\\ C_B^{\mathrm{u}} &\equiv \max_{t\in[t^-,t^+]}\max_{|w|\le C_T C_z} |N_{\mathrm{u}} - h_{\mathrm{u}}' N_{\mathrm{s}} - \partial_t h_{\mathrm{u}}|. \end{aligned} \tag{33}$$

Again, solutions of (32) that lie in the stable manifold $W^{\mathrm{s}}(\Gamma)$ satisfy the integral equation

$$\zeta_{\mathrm{u}}(t)=\int_{\infty}^{t} \mathrm{e}^{\int_\tau^t \lambda(s)\,\mathrm{d}s}[a_{\mathrm{u}}(\zeta(\tau),\tau)\zeta_{\mathrm{u}}(\tau)+B_{\mathrm{u}}(\zeta(\tau),\tau)]. \tag{34}$$

Since the kinematic eddy boundary near $W^{\mathrm{s}}_{\mathrm{loc}}(\Gamma)$ satisfies $\zeta_{\mathrm{u}}\equiv 0$, its distance from the local stable manifold of Γ can be defined as

$$\mathrm{d}_{\mathrm{s}}=\sup_{t\in[t^-,t^+]}\sup_{\zeta(0)\in W^{\mathrm{s}}_{\mathrm{loc}}(\Gamma)} |\zeta_{\mathrm{u}}(t)|.$$

Using the integral Eq. (34), and the estimates (33) and (18), we obtain that

$$\mathrm{d}_{\mathrm{s}}\le \frac{\lambda_{\min}}{\lambda_{\min}^2 - C_A^{\mathrm{u}}\lambda_{\min} - \lambda'_{\max}} C_B^{\mathrm{u}}. \tag{35}$$

Similarly, the distance of manifold $W^{\mathrm{u}}_{\mathrm{loc}}(\Gamma)$ from the eddy boundary can be defined as

$$\mathrm{d}_{\mathrm{u}}=\sup_{t\in[t^-,t^+]}\sup_{\zeta(0)\in W^{\mathrm{u}}_{\mathrm{loc}}(\Gamma)} |\zeta_{\mathrm{s}}(t)|,$$

which in turn can be estimated as

$$\mathrm{d}_{\mathrm{u}}\le \frac{\lambda_{\min}}{\lambda_{\min}^2 - C_A^{\mathrm{s}}\lambda_{\min} - \lambda'_{\max}} C_B^{\mathrm{s}}. \tag{36}$$

using a similar argument.

As a second step, we now extend the local estimates to global estimates for the distance of the manifolds $W^{\mathrm{s}}(\Gamma)$ and $W^{u}(\Gamma)$ from the eddy boundary Φ. Let $\Delta\tau(t_0)$ denote the time that an "Eulerian" solution $v(t;t_0)=(x(t),y(t))$ on ϕ_{t_0} spends outside a C_z-neighborhood of the stagnation point $u(t_0)$. (Note that $v(t;t_0)$ is the general not a solution of the original Eq. (1), but it does give a parametrization of the kinematic eddy boundary in terms of the parameters t and t_0). Let $C_v>0$ be such that the orbit ϕ_{t_0} is contained in the C_v-neighborhood of $u(t_0)$ for every t_0. Since the velocity field (1) is smooth, for $|v|, |\bar{v}|\le C_v$ we can write

$$|f(v,t)-f(\bar{v},\bar{t})|=L_1|v-\bar{v}|+L_2|t-\bar{t}|,$$

with the Lipschitz constants

$$L_1 = 2 \max_i \max_{t\in[t^-,t^+]} \max_{|v|\le C_v} |\nabla f_i(v,t)|,$$
$$L_2 = 2 \max_i \max_{t\in[t^-,t^+]} \max_{|v|\le C_v} |\partial_t f_i(v,t)|.$$

Let us now consider a solution $X(t) = (x(t), y(t)) \in W^{\mathrm{u}}(\Gamma)$, $t \in [t^-, t^+]$. The distance of this solution from a solution $v(t; t_0)$ on the homoclinic set Φ obeys the estimate

$$\begin{aligned}
|X(t) - v(t;t_0)| &\le |X(t_0) - v(t_0;t_0)| + \int_{t_0}^{t} |f(X(\tau),\tau) - f(v(\tau;t_0),t_0)|\,\mathrm{d}\tau \\
&\le |X(t_0) - v(t_0;t_0)| + \int_{t_0}^{t} |f(X(\tau),\tau) - f(v(\tau;t_0),\tau)|\,\mathrm{d}\tau \\
&\quad + \int_{t_0}^{t} |f(v(\tau;t_0),t) - f(v(\tau;t_0),t_0)|\,\mathrm{d}\tau \\
&\le |X(t_0) - v(t_0;t_0)| + L_2(t-t_0) + \int_{t_0}^{t} L_1 |X(\tau) - v(\tau;t_0)|\,\mathrm{d}\tau,
\end{aligned}$$

which, by Gronwall's inequality, implies that for any $t \in [t_0, t_0 + \Delta\tau(t_0)]$,

$$|X(t) - v(t;t_0)| \le [|X(t_0) - v(t_0;t_0)| + L_2\Delta\tau(t_0)]\mathrm{e}^{L_1\Delta\tau(t_0)}. \tag{37}$$

This means, e.g., that if we start an actual solution $X(t)$ δ-close to the homoclinic loop ϕ_{t_0}, then it stays within a distance of

$$2\delta\mathrm{e}^{L_1\Delta\tau(t_0)}$$

from the homoclinic loop outside a C_z-neighborhood of the stagnation point $u(t_0)$ provided the time-dependence of the vector field is "slow enough" so that $L_2 \le \delta/\Delta\tau(t_0)$ holds.

Let $l(t_0)$ denote the arclength of the part of the homoclinic loop ϕ_{t_0} that falls outside the C_z neighborhood of the stagnation point $u(t_0)$, and let

$$\Delta T = \max_{t_0\in[t^-,t^+]} \max_{|p-u(t_0)|\ge C_z, p\in\phi_{t_0}} \frac{l(t_0)}{|\nabla\psi(p,t_0)|}.$$

It is easy to see that ΔT provides a uniform upper estimate for the Eulerian "flight times" $\Delta\tau(t_0)$. Then using the estimates (36), (37), we can conclude the following:

Theorem 4.1. Outside the C_z-neighborhood of the stagnation curve $u(t)$, the C^0 distances of the manifolds $W^{\mathrm{u}}(\Gamma)$ and $W^{\mathrm{s}}(\Gamma)$ from the kinematic eddy boundary Φ obey the estimates

$$\mathrm{dist}(W^{\mathrm{u}}(\Gamma),\Phi) \le D_{\mathrm{u}} \equiv \left[\frac{\lambda_{\min}C_B^{\mathrm{s}}}{\lambda_{\min}^2 - C_A^{\mathrm{s}}\lambda_{\min} - \lambda'_{\max}} + L_2\Delta T\right]\mathrm{e}^{L_1\Delta T},$$
$$\mathrm{dist}(W^{\mathrm{s}}(\Gamma),\Phi) \le D_{\mathrm{s}} \equiv \left[\frac{\lambda_{\min}C_B^{\mathrm{u}}}{\lambda_{\min}^2 - C_A^{\mathrm{u}}\lambda_{\min} - \lambda'_{\max}} + L_2\Delta T\right]\mathrm{e}^{L_1\Delta T}.$$

Note that the above estimates yield small numbers if the explicit time dependence of the vector field (1) is slow in a neighborhood of the kinematic eddy boundary Φ.

5. Lagrangian transport from Eulerian observations

We are now in the position to relate the shape of the kinematic eddy boundary (i.e., the deformation of the loops ϕ_{t_0} as the time $t_0 \in [t^-, t^+]$ varies) to the transport of particles between an unbounded and a bounded subset of the physical space (x, y). More precisely, let us assume that the conditions of Theorem 1 hold and hence the locally invariant manifolds Γ, $W^u(\Gamma)$, and $W^s(\Gamma)$ exist. For every $t_0 \in [t^-, t^+]$, define the point $p_{t_0} \in \phi_{t_0}$ which divides the homoclinic loop ϕ_{t_0} into two connected components of equal arclength. Let $N(p_{t_0})$ denote the normal space to ϕ_{t_0} at p_{t_0} embedded in $\mathbb{R}^2$. Out of individual normal spaces we can build the normal surface

$$N(u) = \{(x, y, t_0) | (x, y) \in N(p_{t_0}),\ |(x, y) - p_{t_0}| \leq 2\max(D_u, D_s),\ t_0 \in [t^-, t^+]\}.$$

Let γ^u denote the first intersection of the unstable manifold $W^u(\Gamma)$ with $N(u)$ in backward time, and let γ^s denote the first intersection curve of the stable manifold $W^s(\Gamma)$ with $N(u)$ in backward time. According to our estimates in Theorem 4.1, the two curves γ^u and γ^s are C^0-close to the intersections of the kinematic eddy boundary Φ with $N(u)$. Define the *gate surface* G to be the set of points on $N(u)$ that lie between $W^s(\Gamma)$ and $W^u(\Gamma)$, i.e., between the two curves γ^u and γ^s. (Note that γ^u and γ^s may intersect, in which case the surface G locally shrinks to a point at the time of intersection.) Also, consider the surface $S^u \subset W^u(\Gamma)$ which is bounded by the curves Γ and γ^u, and the surface $S^s \subset W^s(\Gamma)$ bounded by Γ and γ^s. Then the cylindrical surface

$$\mathcal{B} = S^u \cup G \cup S^s$$

is a two-dimensional surface in the extended phase space with a uniquely defined exterior and interior Ext $(\mathcal{B})$ and Int $\mathcal{B}$. We define the *dynamic eddy* $\mathcal{E}$ associated with the kinematic eddy Φ as

$$\mathcal{E} = \text{Int}(\mathcal{B}).$$

The geometry of this construction is shown in Fig. 5. The set $\mathcal{B}$ is referred to as the dynamic eddy boundary. We will use the notation

$$\mathcal{E}_{t_0} = \mathcal{E} \cap \{t = t_0\}$$

for the constant time slices of the dynamic eddy. Initial conditions that enter $\mathcal{E} = \text{Int}(\mathcal{B})$ at some point in the time interval $[t^-, t^+]$ exhibit swirling motion for $t \leq t^+$. Initial conditions that remain in Ext$(\mathcal{B})$ for all $t \in [t^-, t^+]$ move differently as they simply pass by the dynamic eddy. In what follows, we are interested in the flux of initial conditions between these two qualitatively different regions of behavior.

Assume first that the curves γ^u and γ^s do not interested each other. Then the vector field points either inwards or outwards on the entire gate surface G, and hence the dynamic eddy is locally invariant in forward or backward time on the time interval $[t^-, t^+]$. Restricting to the former case, we observe that if $F_{t^-}^t(\cdot)$ denotes the solution operator based at $t_0 = t^-$ for system (1), then the local invariance of $\mathcal{E}$ implies

$$F_{t^-}^t(\mathcal{E}_{t^-}) \subset \mathcal{E}_t \tag{38}$$

for all $t \in [t^-, t^+]$. Now the map $F_{t^-}^t$ is area preserving by the Hamiltonian nature of (1), which gives

$$\text{Area}[F_{t^-}^t(\mathcal{E}_{t^-})] = \text{Area}[\mathcal{E}_{t^-}]. \tag{39}$$

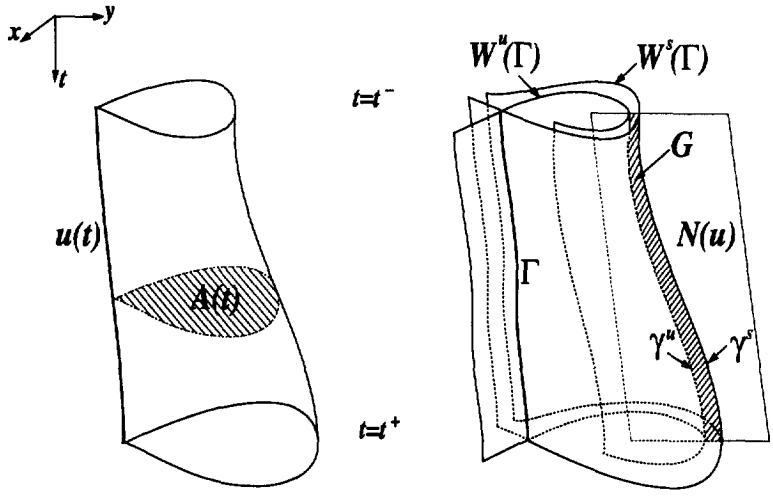

Fig. 5. Kinematic and dynamic eddies.

Formulas (38) and (39) then show that on the time interval $[t^-, t^+]$, the flux of initial conditions into $\mathcal{E}$ obeys the equation

$$\text{Flux}(t) = \frac{\text{Area}[\mathcal{E}_t] - \text{Area}[\mathcal{E}_{t^-}]}{t - t^-}. \tag{40}$$

Let $L(t_0)$ denote the arclength of the homoclinic loop ϕ_{t_0} and let $A(t_0) = \text{Area}[\text{Int}(\phi_{t_0})]$ (see Fig. 5). Then Theorem 4.1 and (40) imply the estimate

$$\left|\text{Flux}(t) - \frac{A(t) - A(t^-)}{t - t^-}\right| \leq \frac{L(t) + L(t^+)}{t - t^-}[D_s + D_u]. \tag{41}$$

A similar argument yields the same formula for the case when the dynamic eddy is locally invariant in backward time, in which case the flux $\text{Flux}(t)$ is a negative number.

Assume now that the curves γ^u and γ^s intersect topologically transversely at the times $t_1, t_2, \ldots, t_n$. Then between two adjacent times of intersection t_k and t_{k+1} an argument identical to the above can be used to establish the estimate

$$\left|\text{Flux}(t) - \text{Flux}(t_k) - \frac{A(t) - A(t_k)}{t - t_k}\right| \leq \frac{L(t) + L(t_k)}{t - t_k}[D_s + D_u]$$

for any $t \in [t_k, t_{k+1}]$. This in turn implies that formula (41) is still valid for the net, signed flux of initial conditions between the times t^- and t with $t \in [t^-, t^+]$. We summarize our results in the following theorem.

Theorem 5.1. Fix a time $t \in [t^-, t^+]$. Then the net, signed flux of particles through the dynamic eddy boundary obeys the estimate

$$\left|\text{Flux}(t) - \frac{A(t) - A(t^-)}{t - t^-}\right| \leq 2\frac{L(t) + L(t^-)}{t - t^-}\left[\frac{\lambda_{\min} C_B}{\lambda_{\min}^2 - C_A\lambda_{\min} - \lambda'_{\max}} + L_2\Delta T\right] e^{L_1\Delta T},$$

where $C_B = \max(C_B^s, C_B^u)$ and $C_A = \max(C_A^s, C_A^u)$.

The above theorem says that the flux into the dynamic eddy is equal to the rate of change of the area of the kinematic eddy plus a correction term. This correction term is small if the rate of change of the eddy size is small.

In the limit of infinitesimally slow eddy deformation, the above theorem simplifies to the adiabatic transport results given in [15], where the Melnikov method and Fenichel's invariant manifold theory was used in the calculations. We note that our results do not assume adiabaticity for the flow, and hence do not require the identification of a small parameter in the data set. As we noted in Section 1, the presence of a uniformly small parameter for the entire field (1) usually cannot be expected in real-life flows.

6. A kinematic eddy–jet interaction model

In order to show how the presence of an isolated eddy (Gulf Stream Ring) effects the cross stream mixing of particles in a eastward flowing, two-dimensional jet, Dutkiewicz and Paldor [9] proposed a simple kinematic model for the process. For oceanographically reasonable parameter values, this model produces a transient hyperbolic stagnation point which lies on the boundary of a kinematic eddy. We will use our results from earlier sections to predict the presence of a dynamic eddy in the flow and also give estimates for the Lagrangian flux associated with the transport between the eddy and the jet. Although the model is given analytically in terms of a streamfunction, we will compute the necessary Eulerian quantities on a grid as one would do for a numerically or experimentally generated Eulerian field. Our study is a continuation of that of Haller and Poje [13] where the adiabatic limit of the same problem was considered with parameter values producing a permanent kinematic eddy.

In the model of Dutkiewicz and Paldor, the meandering jet flow of Bower [6] is superimposed on a Gaussian eddy and, while the resulting velocity field is a purely kinematic approximation, the model provides an explicit oceanographic example in which the accuracy and applicability of the preceding mathematical ideas can be illustrated. Using the notation of [9], the eddy–jet interaction model results from the the superposition of two streamfunctions which can be written as

$$\begin{aligned} \psi_{\text{jet}}(x, y, t) &= J \tanh\left\{\frac{1}{L}(y - A\sin[k(x - ct)])\right\}, \\ \psi_{\text{eddy}}(x, y, t) &= E \exp\left\{-\frac{1}{2\sigma^2}[(x - \mu_x)^2 + (y - \mu_y)^2]\right\}. \end{aligned} \tag{42}$$

We choose the parameters to model typical Gulf Stream observations:

$$\begin{aligned} &J = 6.0\,\text{km}^2/\text{min}, \qquad E = 4.5\,\text{km}^2/\text{min}, \\ &L = 50\,\text{km}, \quad A = 60\,\text{km}, \quad \sigma^2 = 625.0\,\text{km}^2, \quad k = 0.0157\,\text{km}^{-1}. \end{aligned}$$

Varying the meander speed c, allows us control over the time rate of change of the Eulerian stagnation point and its linearization. We study the Lagrangian dynamics for three different values of c: (Case 1) $c = 60\,\text{km/day}$, (Case 2) $c = 12(\text{km/day})$ and (Case 3) $c = 6\text{km/day}$. For the Gulf Stream, we have $c \approx 10\,\text{km/day}$. In this particular example, the topology of the Eulerian snapshots is unchanged by the magnitude of c; only the value of time at which the snapshot is taken is effected.

Fig. 6 shows the combined streamfunction at four different values of the time index $t = L_t/c$ with the constant L_t to be defined later. In Fig. 7 the location of the Eulerian stagnation point (crosses) and the shape of the instantaneous kinematic eddy boundaries are shown for times during the period of interest.

We note that while the flow is temporally periodic, we are only concerned with the dynamics during a specific part of the period and make no use of the periodicity in the calculations.

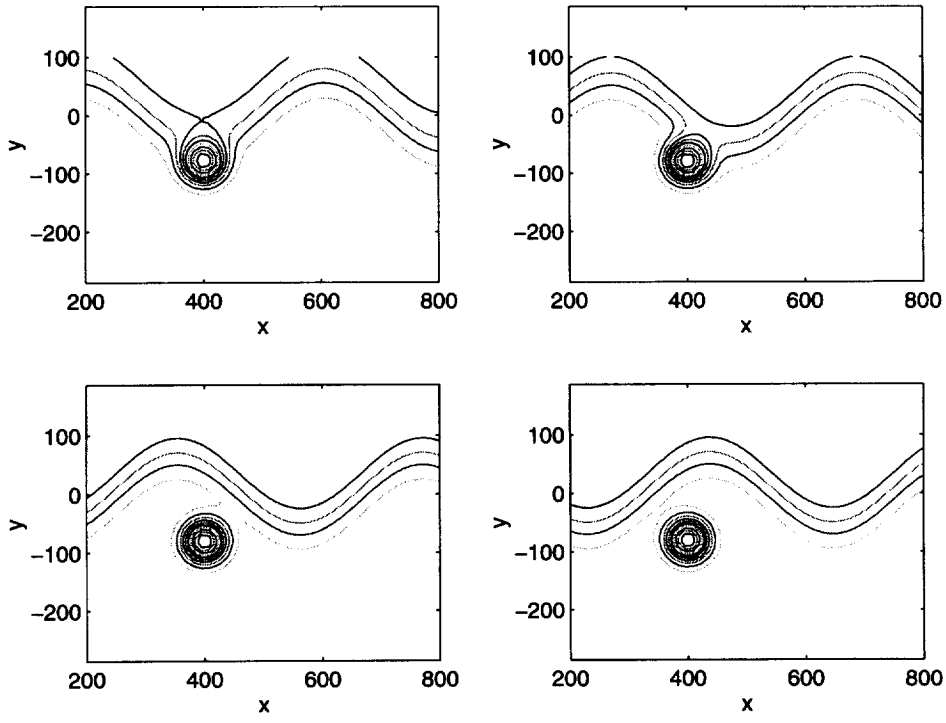

Fig. 6. Combined streamfunction, $\psi_{\text{jet}} + \psi_{\text{eddy}}$, at four different times during the period.

6.1. *Verification of inequalities*

The velocity fields generated by (42) were discretized in space on a square grid with resolution $\Delta x = 0.25\,\text{km}$. Centered difference approximations of the flow produced (see (30))

$$\bar{C} = L_F = C_z C_f \approx 1.5 \times 10^{-4}\,\text{km}^{-1}\,\text{min}^{-1},$$

where the radius $C_z = 5\,\text{km}$ around the Eulerian stagnation point was chosen to satisfy the above approximation. The values of the Eulerian quantities $(\lambda, \dot{\lambda}, \dot{u}, \ldots)$ were calculated at 12 times in the interval, and we selected

$$t_- = L_t/c, \qquad t_+ = t_i + L_t/2c$$

with the constant $L_t \approx 166\,\text{km}$.

We verified the conditions in (31) of Theorem 3.1 for three different values of the meander speed, the results are shown in Figs. 8–10 as functions of time after three initial times in the interval $t \in [t_-, t_+]$.

We rewrite two of the three inequalities (31) as

$$\begin{aligned} &\lambda_{\min}^2 > \lambda'_{\max} + 2C_T\lambda_{\min}(C_T^2\bar{C} + C'_T) = \Lambda_{\max}, \\ &|\dot{u}|_{\max} = \mu < \left[\frac{\lambda_{\min}^2 - \lambda'_{\max}}{2C_T\lambda_{\min}} - C'_T\right] = U. \end{aligned} \tag{43}$$

We found numerically that the second inequality in (31) is always satisfied if the third one is satisfied, therefore we will only be concerned with the inequalities listed in (43). The first of these places a limit on the time rate of

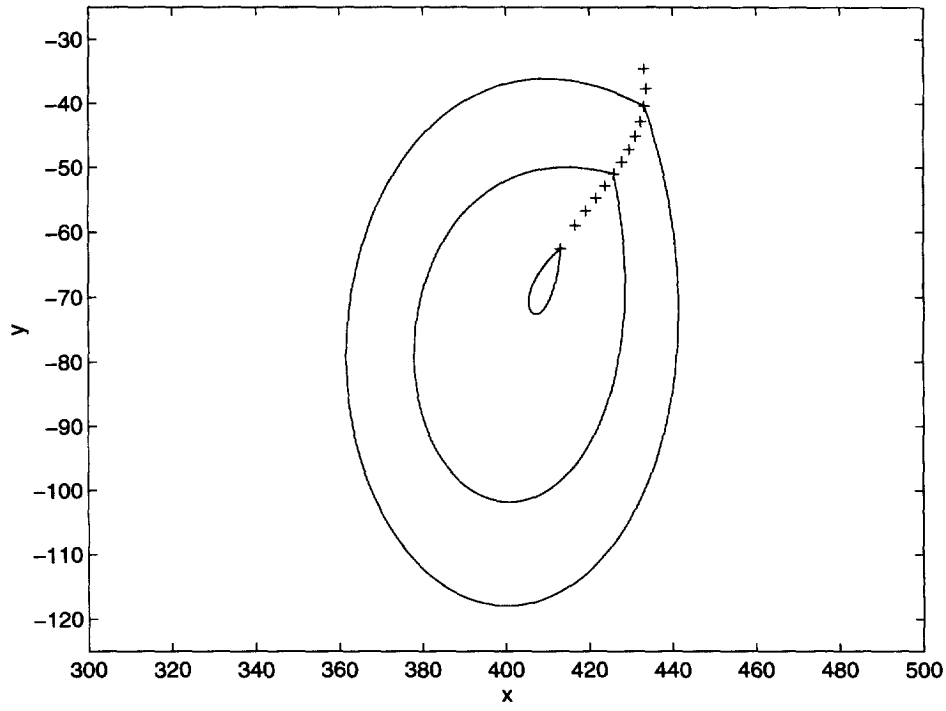

Fig. 7. Location of stagnation point, (+), and shape of the kinematic eddy at different times in the period.

change of the eigenvalues and eigenvectors. The second limits the speed of the Eulerian stagnation point compared to a measure of the strength of the hyperbolicity. We plot both sides of the inequalities as functions of time take the running maximum or minimum of the indicated quantities.

In the first case (see Fig. 8), where the Eulerian structures move at unrealistically high speeds, there exist some initial times after which the first set of estimates are satisfied; $|\dot{u}|_{\max}$ is, however, always greater than U. We do not expect to be able to construct meaningful Lagrangian hyperbolic structures in this case.

As the meander speed is reduced, the estimates for both $\dot{\lambda}$ and $\mu = |\dot{u}|_{\max}$ are satisfied on open intervals of time for the proper choice of initial time. Without doing any extensive optimization, the results in Fig. 9 prove that a hyperbolic Lagrangian trajectory exists for at least several days during the period of interest. Further reduction in the meander speed (see Fig. 10) increases the length of the time interval in which the estimates are satisfied.

6.2. *Invariant manifolds*

We compute numerical approximations to the local stable and unstable manifolds using the "straddling" techniques of Miller et al. [22]. Using the appropriate time slice of the kinematic eddy boundary as a template, a short segment of initial conditions is aligned in the unstable direction straddling the stagnation point. These initial conditions are iterated forward in time under the full flow starting from time $t = t_-$ and, as time progresses, new points are added to maintain a constant density of points on the growing line. An approximation to the local stable manifold is arrived at in a similar way; initializing a short line segment in the stable direction at time $t = t_+$ and evolving these initial conditions backward in time. Depending on the strength of the local saddle dynamics, this method has been shown to be a robust numerical technique for 2D manifold computations (see [25]).

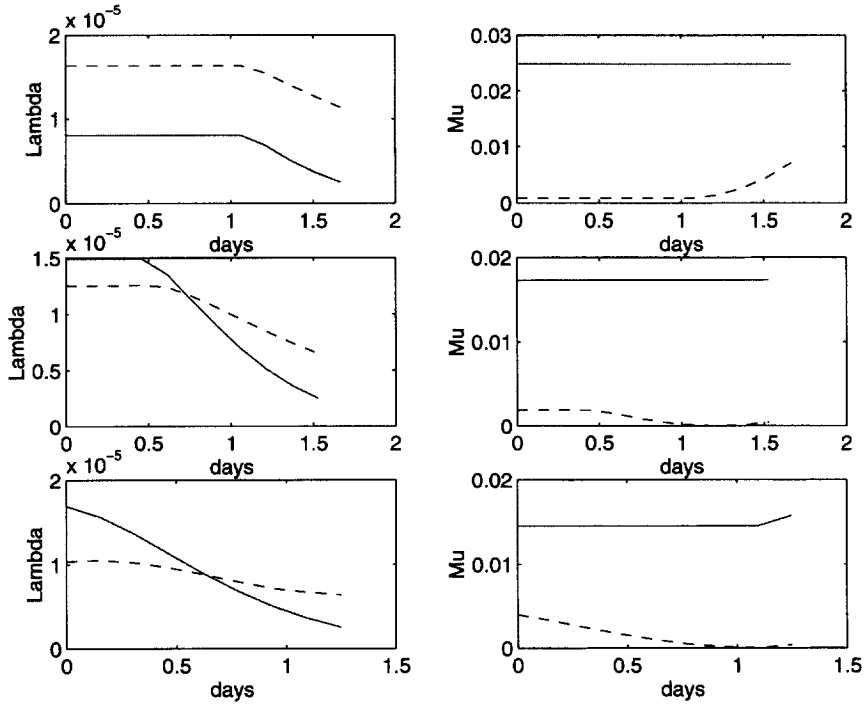

Fig. 8. Estimates at three different initial times for Case 1: $c = 60$Km/day. On the left, $\lambda^2_{\min}(t)$ solid, $\Lambda_{\max}(t)$ dashed. On the right, $\mu = \dot{\mu}_{\max}(t)$ solid, $U(t)$, dashed.

We show the time slices of manifolds computed in this way in Fig. 11 at three different times for each of the three values of the meander speed. In the case of fast structure speed, Fig. 11(a), the time scale of the saddle dynamics is comparable to the total time of interest. The resulting manifolds remain short line segments revealing little about the underlying Lagrangian dynamics. For the more realistic meander speeds shown in Figs. 11(b) and (c), the conditions of Theorem 3.1 are satisfied and we expect to compute meaningful approximations to the finite-time stable and unstable manifolds. These manifolds do not exhibit homoclinic tangles and the resulting lobes associated with chaotic dynamics. Instead, since the size of the kinematic eddy is growing monotonically during the time of observation, the stable and unstable manifolds intersect only at the hyperbolic solution $\Gamma(t)$; the exchange of fluid is unidirectional from the jet into the eddy. At any given time, the initial conditions in the jet that eventually find their way into the recirculating dynamic eddy are given by those points that lie within the "mixing channel" bordered by the two segments of the finite-time stable manifold.

The nature of the Lagrangian dynamics in the eddy neighborhood is most easily viewed in the extended three-dimensional phase space where time $z = t$, is the third dimension. In this space, the approximate manifolds are two-dimensional, invariant sheets as shown in Fig. 12, where for clarity, only clipped segments of $W^s(\Gamma)$ and $W^u(\Gamma)$ are shown. Particles initiated within the tubular region defined by $W^s(\Gamma)$ evolve (the time axis is positive down) into the recirculating region given by the spiraling sheet of $W^u(\Gamma)$. All other initial points bypass the dynamic eddy.

The relation between the approximate location of the Lagrangian hyperbolic trajectory, $\Gamma(t)$ and the fixed time Eulerian stagnation point is shown in Fig. 13. As we stated in Theorem 3.1, the Eulerian picture provides an increasingly accurate indicator of the distinguished Lagrangian orbit as the speed of the Eulerian structures is reduced.

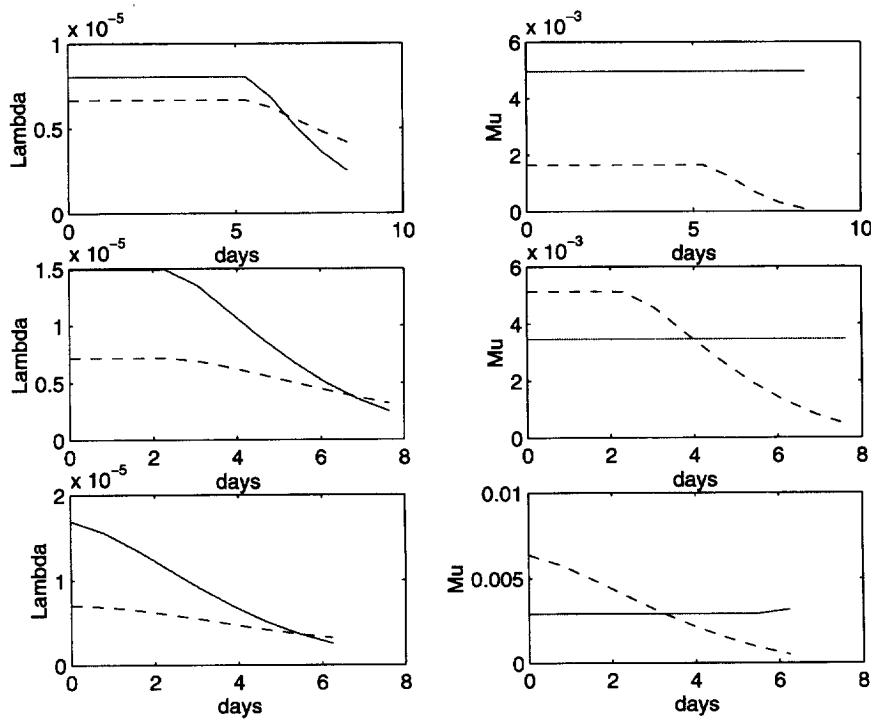

Fig. 9. Estimates at three different initial times for Case 2: $c = 12\,\mathrm{km/day}$. Legend as in Fig. 8.

To illustrate the non-uniqueness of finite-time invariant manifolds, we perturb the position of the initial line segment used to compute the unstable manifold. The approximate $W^{\mathrm{u}}(\Gamma)$'s shown in Fig. 14 were computed using a line of initial conditions with endpoints,

$$(x_1, y_1) = (407.0, -67.0), \qquad (x_2, y_2) = (429.0, -58.0).$$

We expect that the shape of the manifolds should, in the case of sufficiently strong hyperbolicity, be insensitive to the exact form of the initial conditions. Statement (v) of Theorem 3.1 shows that the manifolds are unique up to an exponential factor given by $\exp(-\bar{\lambda}\tau)$ where $\bar{\lambda}$ is the time averaged eigenvalue of the stagnation point during the time of interest $\tau = t^+ - t^-$. The robustness of the manifolds with respect to initial conditions is a requirement for "real", numerically generated data sets which are typically noisy and spatially under-resolved. Fig. 14 shows time slices $W^{\mathrm{s}}(\Gamma)$ resulting from the above initial line segment and a perturbed line segment with endpoints,

$$(x_1, \tilde{y}_1) = (407.0, -57.0), \qquad (x_2, \tilde{y}_2) = (429.0, -48.0).$$

The upper plots of Fig. 14 show two time slices of the original $W^{\mathrm{u}}(\Gamma)$ (solid) and the perturbed $\tilde{W}^{\mathrm{u}}(\Gamma)$ (dot–dashed) for the case where $c = 120\,\mathrm{km/day}$. For this high meander speed, the conditions of Theorem 3.1 are not satisfied and hence we cannot conclude that a distinguished hyperbolic trajectory exists in the Lagrangian flow. $W^{\mathrm{u}}(\Gamma)$ and $\tilde{W}^{\mathrm{u}}(\Gamma)$ remain well separated throughout the time period indicating weak hyperbolicity and lack of uniqueness. Table 1 gives the "uniqueness" parameter for different meander speeds. It is apparent that, for oceanographically reasonable structure speeds, the computed manifolds are unique up to an immeasurably small error. This is illustrated in the lower two plots of Fig. 14 for the case where $c = 12\,\mathrm{km/day}$. Here $W^{\mathrm{u}}(\Gamma)$ and $(\tilde{W})^{\mathrm{u}}(\Gamma)$ are visually identical in the region near the hyperbolic point $\Gamma(t)$.

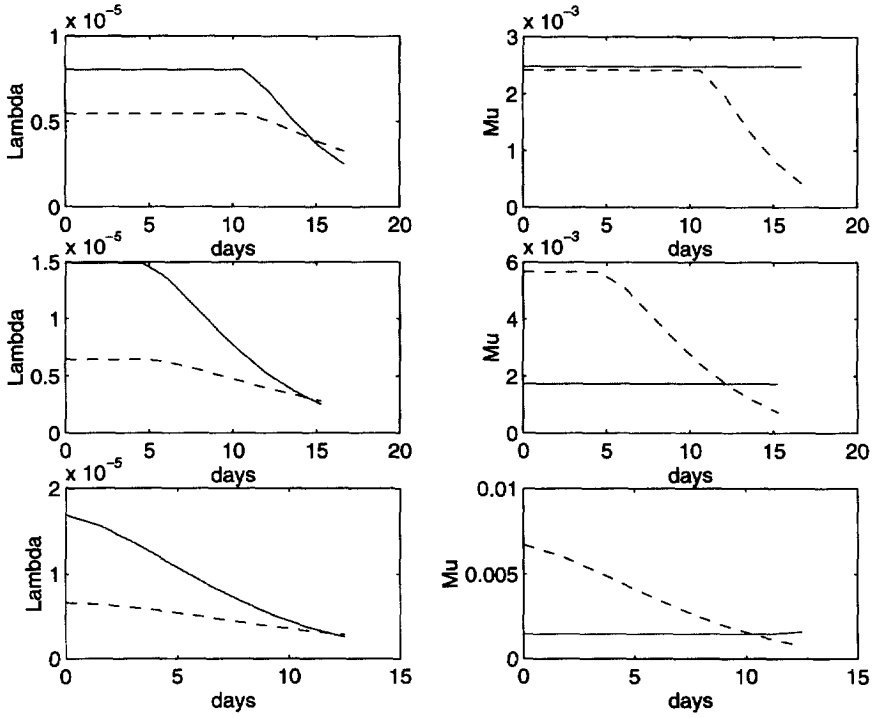

Fig. 10. Estimates at three different initial times for Case 3: $c = 6\,\mathrm{km/day}$. Legend as in Fig. 8.

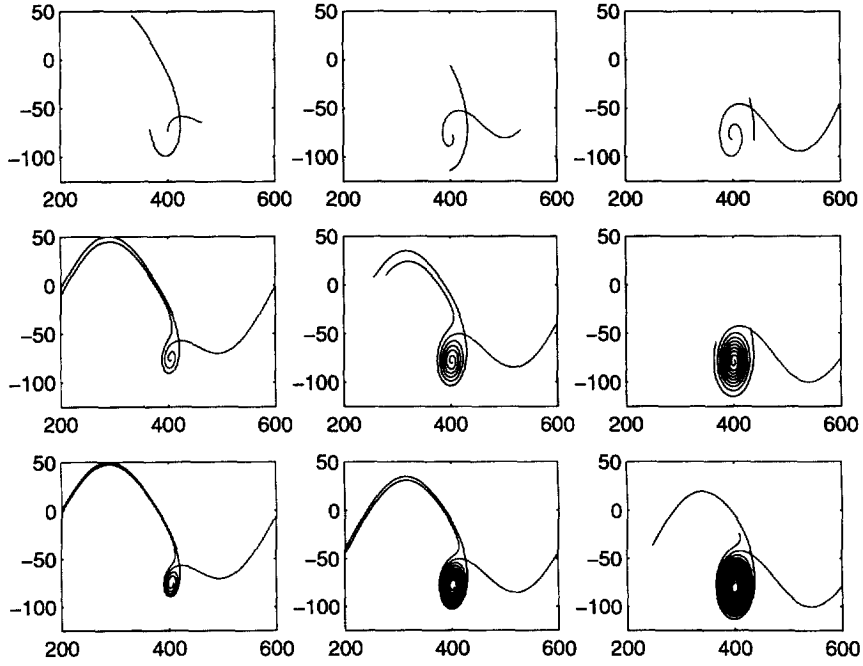

Fig. 11. Time slices of the stable and unstable manifolds for the three meander speeds at three different times. Top, Case 1. Middle, Case 2. Lower, Case 3.

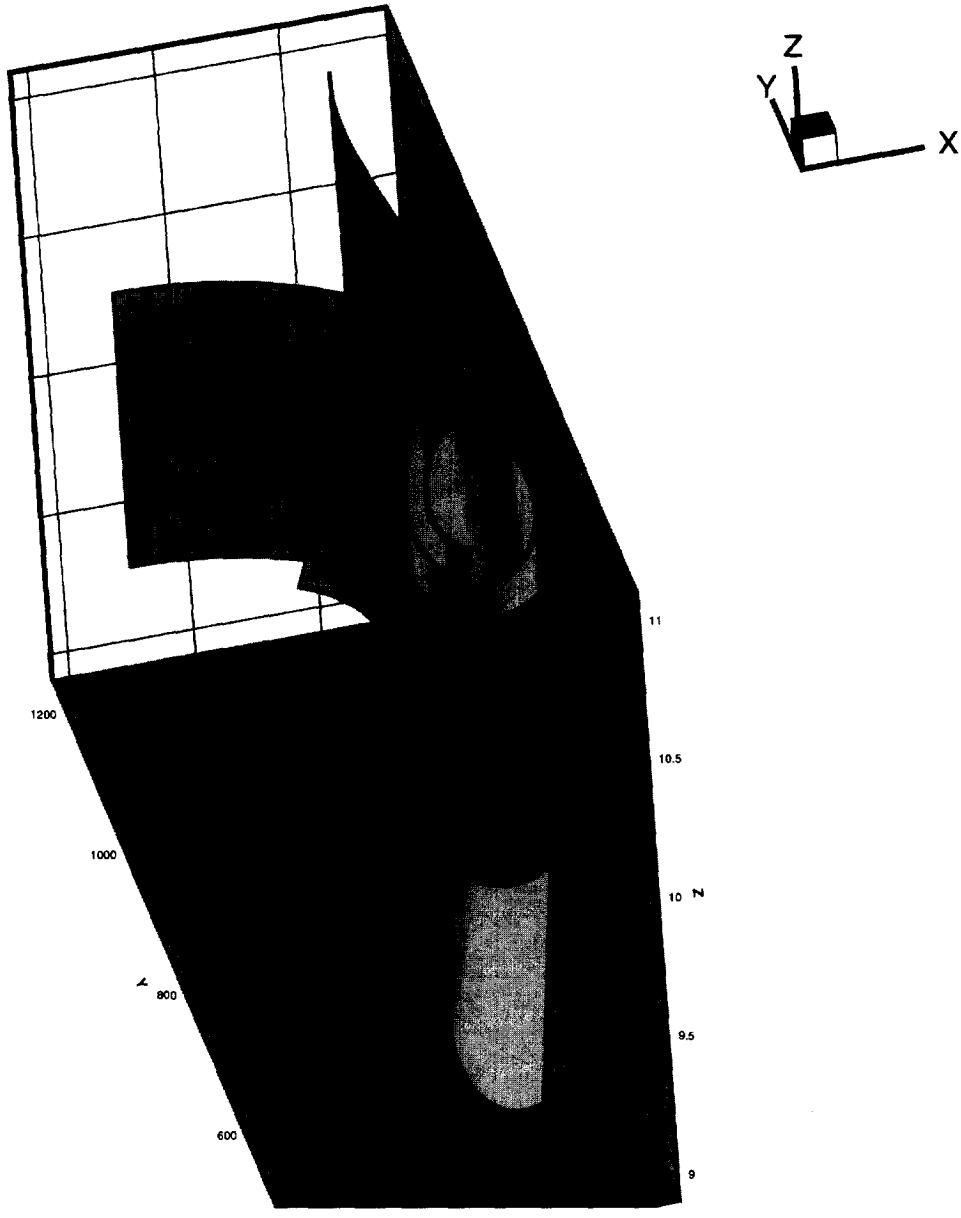

Fig. 12. The stable and unstable manifolds of $\Gamma(t)$ in the extended phase space.

6.3. Transport

Once the finite-time invariant manifolds bounding the dynamic eddy are computed, the flux of fluid particles into the eddy is easily calculated. Fig. 15 shows the geometry of the transport calculations. A constant time segment of the gate surface G introduced in Section 5 is shown in Fig. 15. This line segment, a vertical line at $x = 400$ in Fig. 15, along with the computed manifolds defines an enclosed area. The time rate of change of this area then determines the flux of fluid into or out of the dynamic eddy.

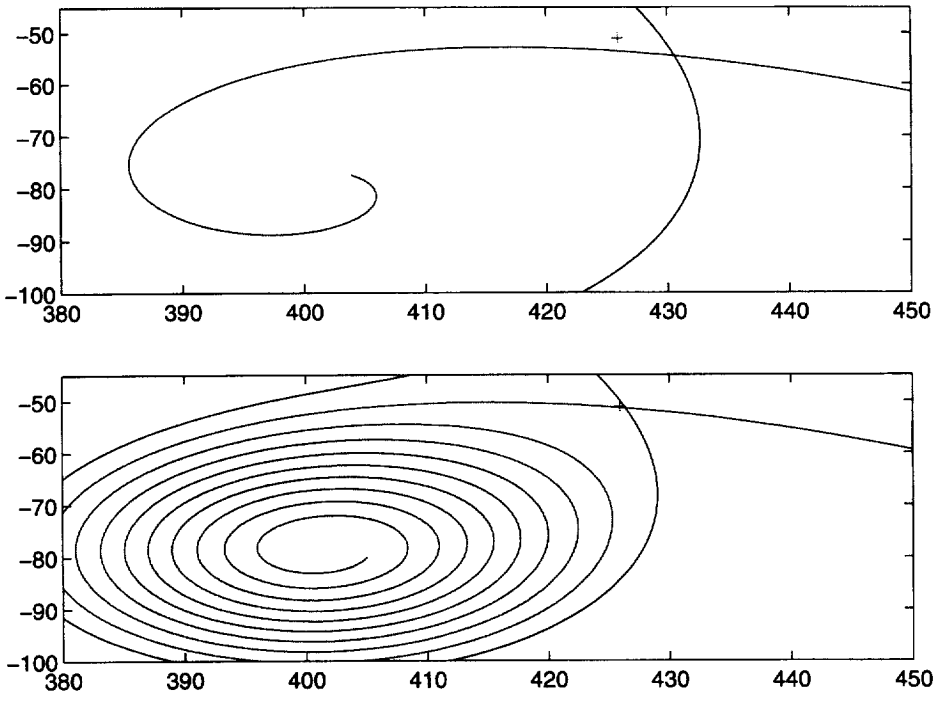

Fig. 13. Location of hyperbolic trajectory, $\Gamma(t)$ and the stagnation point for Case 1, upper and Case 3, lower.

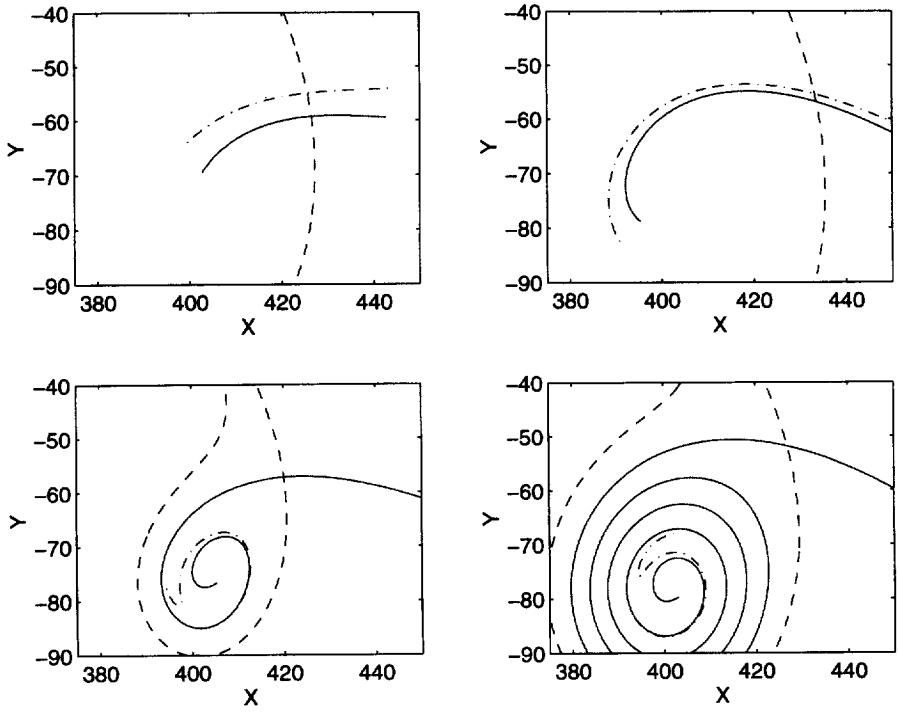

Fig. 14. Non-uniqueness of approximate W^{u}. Top: $c = 120$km/day at times $t = 183\,\mathrm{km}/c$ (left), $t = 208\,\mathrm{km}/c$. Bottom: $c = 12\,\mathrm{km/day}$.

Table 1
Uniqueness parameter, $\bar{\lambda}\tau$ for different meander speeds c

Meander speed km/day)	$\tau = (t^+ - t^-)$(min)	$\bar{\lambda}\tau$	$\exp[-\bar{\lambda}\tau]$
120	1000	3.0	0.052
60	2000	6.0	0.0027
12	10000	30.0	1.3×10^{-13}

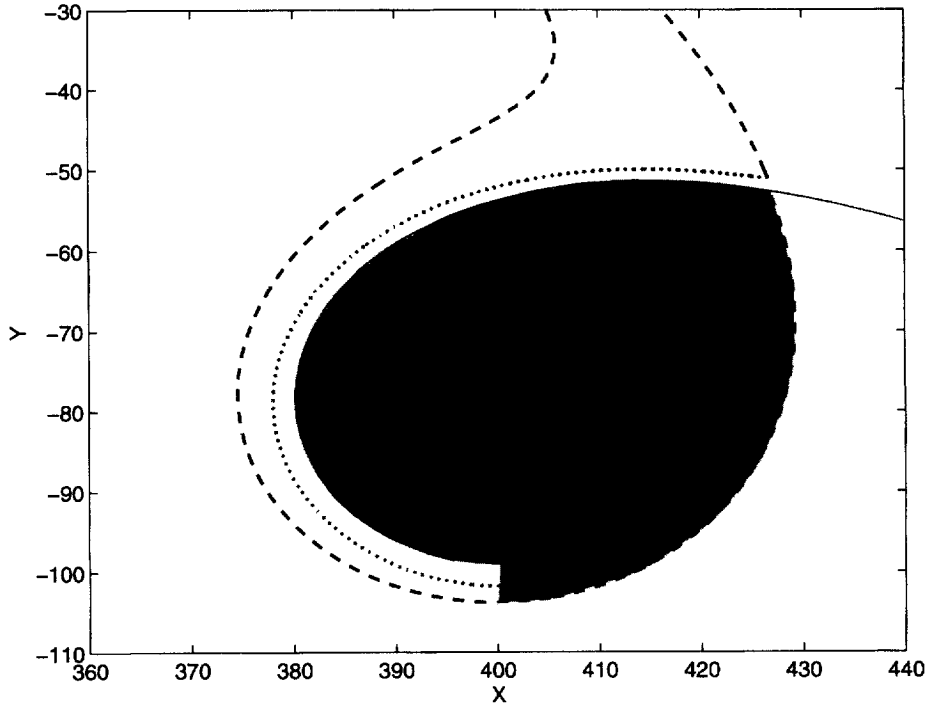

Fig. 15. Mixing geometry for the finite time 'eddy': (—), W^s, (. . .), kinematic 'eddy'; (–), W^u; dynamic eddy area shown shaded.

Table 2
Eulerian versus Lagrangian fluid flux. (The initial and final times were chosen as $t_1 = 183.333$ km/c, $t_3 = 225$ km/c)

Meander speed (km/day)	$F_L^{1,3}$(Sv)	$F_E^{1,3}$(Sv)	Difference (%)
30	10.3	10.9	5.5
12	4.20	4.36	3.7
6	2.14	2.18	1.8
3	1.08	1.09	0.9

Table 2 compares the Lagrangian flux, F_L, calculated from the computed manifolds to the flux F_E calculated from area differences of the time slices of the kinematic eddy boundary. In order to standardize the units, we assume a layer depth of 500 meters and define the flux between two times (a, b) as

$$F^{a,b} = 500 * \frac{A(t_b) - A(t_a)}{(t_b - t_a)}$$

in a oceanographic units of Sverdrups, $1Sv = 10^6 m^3/s$.

We conclude from this table that the Eulerian calculation given in Theorem 5.1 provides a very good approximation for the rate of Lagrangian into the dynamic eddy. As stated in Theorem 5.1, the difference in fluxes computed from the Eulerian and Lagrangian structures becomes negligible as the speed of the structures approaches zero.

7. Conclusions

In this paper we developed a theory of Lagrangian mixing for two-dimensional Hamiltonian systems with general time-dependence. Theorem 3.1 gives conditions under which a finite-time kinematic eddy in the contour plot of the Hamiltonian gives rise to a dynamical eddy in the actual flow. The dynamical eddy is encircled by the stable and unstable manifolds of a solution, which is hyperbolic on a finite-time interval. In Theorem 5.1 we gave an estimate for the flux of initial conditions between the eddy and its environment based on quantities computed from the Hamiltonian ψ. Although our results do not assume the presence of a small parameter in the Hamiltonian, they can be used in near-integrable or adiabatic problems to estimate the maximal value of the perturbation parameter for which the flow still admits a hyperbolic solution with stable and unstable manifolds. Furthermore, the flux estimate given in Theorem 5.1 simplifies to that given in [15] in the case of adiabatic systems. In this sense, earlier results on two-dimensional flows with small parameters and special time-dependence can be derived as special cases of our theory. The exception is the flux calculation for near-integrable Hamiltonians of the form $\psi_0(x, y) + \epsilon\psi_1(x, y, t)$, where the flux estimate of Theorem 5.1 may be crude compared to an exact Melnikov calculation for lobe areas. (Note that for periodic and quasiperiodic flows, our definition of the flux in (40) is just the same as the one used in lobe dynamics, since the invariant manifolds of the appropriate Poincaré maps are just $t = \text{const.}$ slices of our invariant manifolds.)

We note that our results also apply to three-dimensional unsteady flows with a continuous, volume-preserving symmetry. As shown in [12], such flows can be reduced to two-dimensional Hamiltonian systems, and hence the theory in this paper can be applied.

Finally, we point out that based on Theorems 3.1 and 5.1, it is straightforward to design numerical algorithm that identify potential Lagrangian mixing regions in a given data set, estimate the location and lifespan of the underlying hyperbolic structures and the flux of initial conditions. Such calculations will appear in [24], where the ideas developed in this paper are applied to the numerically generated vector field of a barotropic, double gyre ocean model.

Acknowledgements

We would like to thank Pat Miller for introducing us to his results and for his useful suggestions. We are grateful to Chris Jones and Vered Rom-Kedar for several helpful remarks.

References

[1] H.S. Balasuriya, C.K.R.T. Jones, B. Sandstede, Viscous perturbations of vorticity-conserving flows and splitting of separatrices, Nonlinearity 11 (1998) 47–77.

[2] D. Beigie, Codimension-one partitioning in multi-degree-of-freedom Hamiltonian systems with non-toroidal invariant manifold intersections, Preprint, 1994.

[3] D. Beigie, Multiple separatrix crossing in multi-degree-of-freedom Hamiltonian flows, Preprint, 1994.

[4] D. Beigie, A. Leonard, S. Wiggins, Chaotic transport in the homoclinic and heteroclinic tangle regions of quasi-periodically forced two-dimensional dynamical systems, Nonlinearity 4 (1991) 775–819.

[5] D. Beigie, A. Leonard, S. Wiggins, The dynamics associated with the chaotic tangles of two-dimensional quasiperiodic vector fields Theory and applications, in: F.G. Carnevale, R. Pierrehumbert (Eds.), Nonlinear Phenomena in Atmospheric Oceanic Sciences, IMA Volumes in Mathematics and Applications, vol. 40, Springer, New York, 1992, pp. 47–138.
[6] A.S. Bower, A simple kinematic mechanism for mixing fluid parcels across a meandering jet, J. Phys. Oceanogr. 21 (1991) 173–180.
[7] R. Camassa, S. Wiggins, Chaotic advection in a Rayleigh–Bénard flow, Phys. Rev. A 43 (1991) 774–797.
[8] J.Q. Duan, S. Wiggins, Fluid exchange across a meandering jet with quasi-periodic variability, J. Phys. Oceanogr. 26 (1996) 1176–1188.
[9] S. Dutkiewitz, N. Paldor, On the mixing enhancement in a meandering jet due to the interaction with an eddy, J. Phys. Oceanogr. 24 (1994) 2418–2423.
[10] M. Feingold, L.P. Kadanoff, O. Piro, Passive scalars, three-dimensional volume preserving maps, and chaos, J. Stat. Phys. 50 (1988) 529–565.
[11] N. Fenichel, Persistence and smoothness for invariant manifolds for flows, Indiana Univ. Math. 21 (1971) 193–225.
[12] G. Haller, I. Mezić, Reduction of three-dimensional, volume-preserving flows with symmetry, Nonlinearity 11 (1998) 319–339.
[13] G. Haller, A. Poje, Eddy growth and mixing in mesoscale oceanographic flows, Nonlin. Proc. Geophys., submitted.
[14] P. Holmes, Some remarks on chaotic particle paths in time-periodic, three-dimensional swirling flows, Contemp. Math. 28 (1984) 393–404.
[15] T.J. Kaper, G.A. Kovačič, A geometric criterion for adiabatic chaos, J. Math. Phys. 35 (3) (1994) 1202–1218.
[16] T.J. Kaper, S. Wiggins, Lobe area in adiabatic Hamiltonian systems, Physica D 51 (1991) 205–212.
[17] Y.T. Lau, J.M. Finn, Dynamics of a three-dimensional incompressible flow with a stagnation point, Physica D 5 (1992) 283–310.
[18] R.S. MacKay, Transport in three-dimensional volume-preserving flows, J. Nonlinear Sci. 4 (1994) 329–354.
[19] R.S. MacKay, J.D. Meiss, I.C. Percival, Transport in Hamiltonian systems, Physica D 13 (1984) 55–81.
[20] K.R. Meyer, G.R. Sell, Melnikov bundles, and almost periodic perturbations, Trans. Am. Math. Soc. 314 (1991) 63–105.
[21] I. Mezić, S. Wiggins, On the integrability and perturbation of three-dimensional fluid flows with symmetry, J. Nonlinear. Sci. 4 (1994) 157–194.
[22] P.D. Miller, C.K.R.T. Jones, A.M. Rogerson, L.J. Pratt, Quantifying transport in numerically generated velocity fields, Physica D 110 (1997) 105–122.
[23] Z. Neufeld, T. Tél, Advection in chaotically time-dependent open Flows, Preprint, 1997.
[24] A. Poje, G. Haller, Lagrangian geometry of cross-stream mixing in a double gyre ocean model, J. Phys. Oceanogr., submitted.
[25] A.M. Rogerson, L.J. Pratt, P.D. Miller, C.K.R.T. Jones, J. Biello, J. Chaotic mixing in a barotropic jet, J. Phys. Oceanogr., submitted.
[26] V. Rom-Kedar, Homoclinic tangles-classification and applications, Nonlinearity 7 (1994) 441–473.
[27] V. Rom-Kedar, Secondary homoclinic bifurcation theorems, Chaos 5 (1995) 385–401.
[28] V. Rom-Kedar, A. Leonard, S. Wiggins, An analytical study of transport, mixing, and chaos in an unsteady vortical flow, J. Fluid. Mech. 214 (1990) 347–394.
[29] V. Rom-Kedar, S. Wiggins, Transport in two-dimensional maps, Arch. Rat. Mech. Anal. 109 (1990) 239–298.
[30] J. Scheurle, Chaotic solutions in systems with almost periodic forcing J. Appl. Math. Phys. (ZAMP) 37 (1986) 12–26.
[31] S. Wiggins, Global Bifurcations and Chaos: Analytic Methods, Springer, New York, 1988.
[32] S. Wiggins, On the geometry and transport in phase space-I: Transport in k-degree-of-freedom Hamiltonian systems, $2 \leq k < \infty$ Physica D 44 (1990) 471–501.
[33] S. Wiggins, Chaotic Transport in Dynamical Systems, Springer, New York, 1992.
[34] A.A. Wray, J.C.R. Hunt, Algorithms for classification of turbulent structures, in: H.K. Moffatt, A. Tsinober (Eds.), Topological Fluid Mechanics Cambridge University Press, Cambridge, 1990.
[35] E.M. Ziemniak, C. Jung, T. Tél, Tracer dynamics in open hydrodynamical flows as chaotic scattering, Physica D 44 (1994) 123–146.